

Chemo-mechanical model of a cell as a stochastic active gel

V. Deshpande^a, A. DeSimone^{b,c}, R. McMeeking^{d,e}, P. Recho^f

^aEngineering Department, University of Cambridge, Cambridge, UK

^bScuola Internazionale Superiore di Studi Avanzati, I-34136 Trieste, Italy

^cThe BioRobotics Institute and Department of Excellence in Robotics and A.I., Sant'Anna School for Advanced Studies, I-56127 Pisa, Italy

^dMechanical Engineering and Materials Departments, University of California, Santa Barbara, USA

^eSchool of Engineering, University of Aberdeen, Aberdeen, UK

^fUniversité Grenoble Alpes, Laboratoire Interdisciplinaire de Physique, CNRS, F-38000 Grenoble, France

Abstract

While it is commonly observed that the shape dynamics of mammalian cells can undergo large random fluctuations, theoretical models aiming at capturing cell mechanics often focus on the deterministic part of the motion. In this paper, we present a framework that couples an active gel model of the cell mechanical scaffold with the complex cell metabolic system stochastically delivering the chemical energy needed to sustain an active stress in the scaffold. Our closure assumption setting the magnitude of the fluctuations is that the chemo-mechanical free energy of the cell is controlled at a target homeostatic value. Our model rationalizes the experimental observation that the cell shape fluctuations depend on the mechanical environment that constraints the cell. We apply our framework to the simple case of a cell migrating on a one dimensional track to successfully capture the different regimes of the cell mean square displacement along the track as well as the magnitude of the long time scale effective diffusive motion of the cell.

1. Introduction

The mechanical behavior of an eukaryotic cell is largely controlled by its cytoskeleton, a polymer structure that is fundamentally out of thermodynamic equilibrium. Cytoskeletal processes such as the polymerization turnover of its scaffold and stress-fibre contractility, driven by molecular motors power-strokes, are fuelled by nutrient exchanges of the cell with its environment. Free-energy is released by the hydrolysis of Adenosine Triphosphate (ATP), ultimately serving as the common free-energy source to drive all the mechanically active processes in the cell.

There now exists a very active branch of study broadly known as “active gel physics” that aims to develop a continuum medium deterministic formalism for the transduction of the chemical energy within cells to the mechanics of its cytoskeleton (Prost et al., 2015). The basic idea behind this approach is to perturb the state of the system (defined subsequently) in the vicinity of an assumed equilibrium state. This allows the use of the formalism of linear out-of-equilibrium thermodynamics and the Onsager symmetry relations. Active gel theories of this type typically involve dissipative processes such as viscosity, diffusion, chemical reactions and, importantly, a generalised force that drives the system out of equilibrium. Given that the hydrolysis of ATP is the free-energy source of the molecular motors actuating the cytoskeleton, the natural choice for this generalised force $\Delta\mu$ is the difference in the chemical potentials of ATP and of the product of hydrolysis. In the current active gel theories, this chemical affinity is maintained at a fixed value as an intrinsic property of the cell, although there is strong evidence in terms of cytoskeleton polymerisation (Solon et al., 2007; Engler et al., 2006) and more direct recent measurements (Park et al., 2020) which suggest that the cellular metabolism is modified by the mechanical environment of the cell. Of note, the linear Onsager

Email addresses: vsd20@cam.ac.uk (V. Deshpande), desimone@sissa.it (A. DeSimone), rmcm@engineering.ucsb.edu (R. McMeeking), pierre.recho@univ-grenoble-alpes.fr (P. Recho)

framework is theoretically valid for a system near equilibrium. In the context of active gels, this would imply that $\Delta\mu$ is small compared to $k_B T$, where k_B is the Boltzmann constant and T the absolute temperature. Under physiological conditions $\Delta\mu$ can be on the order of $20k_B T$, and the use of the Onsager framework should therefore be regarded as a general guideline in which specific phenomenological non-linearities between generalised forces and fluxes should be introduced if necessary.

In order to understand some of the assumptions implicit within the active gel theories, consider a typical in-vitro experiment comprising a cell on a substrate immersed in a nutrient-rich medium (nutrient bath); see Fig. 1. While the cell exchanges nutrients (e.g. glucose) and other species (e.g. gases, ions, morphogens) with the surrounding bath, the entire setup is exposed to an external atmosphere and maintained at constant temperature and pressure. The nutrient bath is assumed to be infinite in extent such that it acts as a *chemostat* maintaining the concentrations of nutrients to a constant level. Within the cell, the ATP hydrolysis reaction fueling the molecular motors in the cytoskeleton is happening spontaneously. If the cell were a closed system, the extent of this reaction should relax to equilibrium. However, a complex and highly regulated system, the cellular metabolism, uses nutrients from the bath to constantly recycle the products of hydrolysis back into ATP. In classical active gel theories, the thermodynamic system considered comprises only the cytoskeleton and it is assumed that the metabolic recycling spontaneously adjusts to maintain a constant value of $\Delta\mu$. In this case, the role of metabolism is therefore analogous to a Maxwell daemon constantly delivering ATP to the cytoskeleton and removing ADP when necessary, such that the extent of ATP hydrolysis keeps monotonically increasing. The free energy of the thermodynamic system is therefore bottomless (Recho et al., 2014). As such, this closure assumption creates no theoretical issues other than the fact that an alternative model based on an open system comprising the cell along with its metabolic system that uses the chemical energy in the bath to dynamically allocate the energy resources to the molecular motors might be more insightful.

Our practical motivation to extend the deterministic active gel formalism to incorporate the cell metabolic system stems from the presence of a so-called “biological noise” in the cell dynamics. The fluctuations associated with this noise provide the mechanism for numerous critical biological functions such as the long time-scale spatial exploration of the environment via Brownian-like motility (Stokes et al., 1991; Li et al., 2008) and the nematic ordering of cells which plays an important role in tissue morphogenesis (Gupta et al., 2015). Biological noise manifests itself through non-thermal fluctuations of cytoskeletal filaments (Brangwynne et al., 2007; Nadrowski et al., 2004) which then propagate into fluctuations of cellular level observables including cell shape and cell stresses as typically quantified by its tractions on the substrate (Engler et al., 2006; Solon et al., 2007). These fluctuations are usually measured in terms of the observables’ standard errors which are typically quite large. For example, the variability of the aspect ratio of cells seeded on stiff substrates is on the order of the mean aspect ratio (Prager-Khoutorsky et al., 2011). Moreover, unlike inorganic systems where these errors are associated with observation or other experimental errors, variability in the observations for cells is associated with their intrinsically fluctuating response and depend on the cell chemical and mechanical environment: typically, the variability in the observations decreases with decreasing stiffness of the cell environment (Engler et al., 2006; Prager-Khoutorsky et al., 2011).

There have been numerous attempts to include the effect of biological fluctuations in models for cell dynamics. A lot of them have borrowed the notion of an effective temperature at a long timescale used to describe the motion of grains in granular media (Edwards and Oakeshott, 1989) and extract the effective temperature by either directly fitting to observations (Stokes et al., 1991; Fabry et al., 2001) or by using physical notions such as persistence length (Brangwynne et al., 2007) to then infer an effective temperature. This notion is clearly not related to its standard statistical thermodynamics definition involving the average kinetic energy of some internal degrees of freedom but is an effective way to describe the magnitude of some fluctuations occurring at the microscale in a non-equilibrium system. Such approaches neglect the fact that the biological noise and hence the effective temperature is in fact a function of the cellular environment. Interestingly, some fully deterministic chemomechanical models of the cell behaviour can lead to a spatio-temporal chaotic behaviour whose long timescale dynamics can be characterized by an effective diffusion coefficient (Dreher et al., 2014; Stankevics et al., 2020). Recently, Shishvan et al. (2018) developed a homeostatic ensemble where the effective temperature emerges from the assumption that the cells maximize entropy while maintaining a homeostatic state. This enabled Shishvan et al. (2018) to capture the coupling of the biological noise with the environment in an equilibrium setting, i.e. providing the statistics of observations but not the temporal nature of the noise.

In this paper we extend the active gel approach (Kruse et al., 2005; Jülicher et al., 2007) to include biological noise as a constitutive material property. In particular, we explain how this noise can originate from the complex metabolic

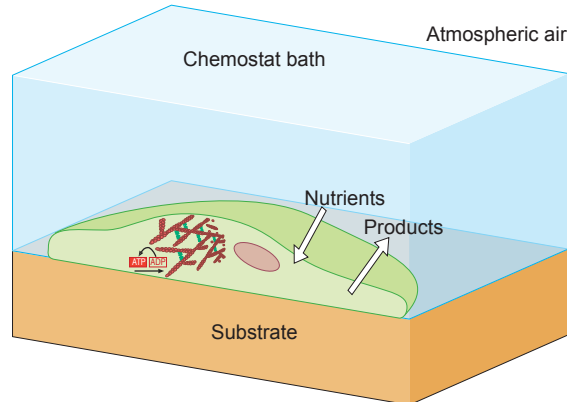


Figure 1: Chemo-mechanical model of the cell. The cytoskeleton filaments are represented in red and cross-linked by molecular motors inflicting active stress in the meshwork. The motors are running by using the chemical energy released during the ATP hydrolysis to ADP. The ADP molecules are recycled into ATP thanks to the cell metabolism that consumes nutrients and expels products. The concentration of nutrients and products in the culture medium is maintained to constant values (chemostat).

pathways that drive the “recharging” of the ATP hydrolysis chemical reaction providing energy to the cytoskeleton. To do so, we assume that the many internal degrees of freedom that control the rate of the recycling process can be described collectively as an equilibrium system producing Brownian noise. The Onsager coupling coefficient between mechanics and hydrolysis leading to the presence of active stress then rationalizes the presence of noise in the mechanical stress and thus in the cell shape as a consequence of the fundamental balance laws. Added to this, because of the Onsager symmetry principle, the mechanical state of the cell also feeds back to the dynamics of the energy delivery producing the active stress. The outcome of this procedure is thus an active gel theory wherein noise not only manifests itself in the active stress but also in the metabolic rate, which becomes inherently coupled to the mechanical environment of the cell.

The paper is constructed as follows. In Section 2, we formulate the mass and momentum conservation laws that characterize the cell mechanical behaviour and build the general thermodynamic framework that we use to derive the constitutive relations of the cell medium. These relations not only involve the connection between stress and deformation in the cell but also describe how the energy is delivered by the cell metabolism to produce an active stress in the system. In Section 3, we introduce our closure assumption that the complex chemical recycling of the metabolites is described by equilibrium fluctuations whose magnitude is fixed to insure that the chemo-mechanical free energy of a cell is controlled to a fixed target. We then reformulate this general stochastic active gel theory in Section 4 for the simple case of a cell crawling on a straight line. By doing so, we obtain three main results that confirm the applicability of the theory. First we demonstrate the dependence of the metabolic activity on the mechanical environment of the cell. Second we show that the resulting cell center of mass mean square displacement is in qualitative agreement with experimental results. Third we compute an effective temperature characterizing the long time scale cell fluctuations that is of the correct order of magnitude. Section 5 gathers our conclusions and outlines some potential generalizations of this work.

2. Close-to-equilibrium thermodynamic framework

The aim of this section is to derive the constitutive behaviour of the cell modeled as an effective continuum medium. The main challenge is to introduce the regulation by the cell metabolism (i.e. rate of energy delivery) of the active stress actuating the cell skeleton. The open thermodynamic system under consideration is constituted of the cell in which only the cytoplasm is modeled and a passive semi-infinite visco-elastic (Kelvin-Voigt) substrate on which the cell is adhering. This whole system can exchange work (W) and heat (Q) with an external bath whose temperature and hydrostatic pressure is fixed but the cell, being an open system, can additionally exchange both energy and matter

with the bath. We assume that the bath sets the constant temperature T of the cell and the substrate and measure all the mechanical stresses in the system with respect to the bath pressure.

The cell occupies the domain ω_t at time t and we denote by $\mathbf{x} \in \omega_t$ the position of a material point within the cell. The set of points $s \in \partial\omega_t$ forms the contour of the cell domain. This contour can be split into two parts: $\partial\omega_t^b$ representing the contact surface of the cell with the bath and $\partial\omega_t^s$ representing the contact surface with the substrate. The semi-infinite substrate occupies the domain Ω_t at time t . Its upper boundary can again be split into two parts with $\partial\Omega_t^c = \partial\omega_t^s$ the contact area with the cell and $\partial\Omega_t^b$ the one with the bath. The rest of the boundary is considered to be static at infinity. The stress-free reference configuration of the substrate (when the cell is absent) is denoted Ω_0 . Material points of the substrate are indexed by the spatial variable $\mathbf{X} \in \Omega_0$ and can be mapped to the actual configuration by $\mathbf{x} = \Psi(\mathbf{X}, t) \in \Omega_t$. Based on such mapping, we can define the substrate deformation tensor $\mathbb{F} = \partial_{\mathbf{X}}\Psi$ and the Green-Lagrange strain tensor $\mathbb{E} = (\mathbb{F}^T\mathbb{F} - \mathbb{1})/2$, where T denotes the transpose operation and $\mathbb{1}$ is the identity tensor.

Conservation laws. We write the first principle of thermodynamics as

$$\dot{U} = \dot{Q} + \dot{W} + \dot{U}_e,$$

where the superimposed dot denotes the time derivative, $U(t)$ is the internal energy of the cell and the substrate and $U_e(t)$ the energy that the cell exchanges with the bath. The entropy balance reads

$$\dot{S} = \frac{\dot{Q}}{T} + \sigma + \dot{S}_e,$$

where $S(t)$ is the entropy of the cell and the substrate, $\sigma(t)$ is the entropy production of the full system and $S_e(t)$ is the entropy which is exchanged between the cell and the bath. The second principle states that the entropy production rate $\sigma \geq 0$. Combining these two principles and defining the Helmholtz free energies $F = U - TS$ -free energy of the cell and its substrate- and $F_e = U_e - TS_e$ -free energy exchanged between the cell and the bath-, we obtain the dissipation

$$\mathcal{D} = T\sigma = \dot{W} + \dot{F}_e - \dot{F} \geq 0.$$

The constitutive equations of the system have to satisfy this fundamental inequality. To compute the dissipation we model the cell cytoskeleton as a continuum medium composed of two phases: a bio-filament meshwork cross-linked by molecular motors that is permeated by a fluid phase, the cytosol. The chemical reactions that are necessary to power the motors take place in the cytosol. Next we write the fundamental balance laws governing the behaviour of such a system.

- *Conservation of momentum.* We denote by $\Sigma(\mathbf{x}, t)$ the total Cauchy stress in the cell. This stress splits into a term associated with the filament meshwork $\mathbb{S}(\mathbf{x}, t)$ and a pressure term associated with the permeating fluid, $P_f(\mathbf{x}, t)\mathbb{1}$:

$$\Sigma = \phi\mathbb{S} - (1 - \phi)P_f\mathbb{1}.$$

In the formula above, $\phi(\mathbf{x}, t)$ denotes the volume fraction of polymer network, which may locally vary. Note that by *a priori* assuming that the stress in the cytosol is purely hydrostatic, we neglect its bulk viscosity compared to the viscous friction of the fluid on the polymer meshwork filaments as often done in poro-elastic theories (Coussy, 2004). We also introduce Σ_s the Cauchy stress tensor in the substrate. We assume that all inertial effects can be neglected such that, denoting ∇ and $\nabla \cdot$ the gradient and divergence operators in the actual configuration, the force balance laws within the cell and substrate read

$$\begin{aligned} -\nabla \cdot ((1 - \phi)P_f) &= -\mathbf{f} \text{ with Boundary Conditions (B.C.) } -(1 - \phi)P_f|_{\partial\omega_t^b} \mathbf{n} = \mathbf{t}_e^P \text{ and } -(1 - \phi)P_f|_{\partial\omega_t^s} \mathbf{n} = \mathbf{0}, \\ \nabla \cdot (\phi\mathbb{S}) &= \mathbf{f} \text{ with B.C. } \phi\mathbb{S}|_{\partial\omega_t^b} \mathbf{n} = \mathbf{t}_e^S \text{ and } \phi\mathbb{S}|_{\partial\omega_t^s} \mathbf{n} = \mathbf{t}_s, \\ \nabla \cdot \Sigma_s &= \mathbf{0} \text{ with B.C. } \Sigma_s|_{\partial\Omega_t^b} \mathbf{n} = \mathbf{0} \text{ and } \Sigma_s|_{\partial\omega_t^s} \mathbf{n} = \mathbf{t}_s, \end{aligned}$$

where $\mathbf{f}(\mathbf{x}, t)$ is the interaction force between the fluid and the polymer, $\mathbf{t}_s(\mathbf{s}, t)$ is the interaction force between the polymer meshwork and the substrate (Parsons et al., 2010), \mathbf{n} the outward unit normal to $\partial\omega_t$ and $\mathbf{t}_e^P(\mathbf{x}, t)$

the traction stress externally applied at the boundary of the cell to the fluid and $\mathbf{t}_e^S(\mathbf{x}, t)$ to the meshwork. These tractions may represent for instance those experimentally applied with an optical trap or an AFM (Suresh, 2007). Therefore the global force balance in the cell and substrate read

$$\nabla \cdot \underline{\Sigma} = 0 \text{ with B.C. } \underline{\Sigma}|_{\partial\omega_t^c} \mathbf{n} = \mathbf{t}_e \text{ and } \underline{\Sigma}|_{\partial\omega_t^s} \mathbf{n} = \mathbf{t}_s, \quad (1)$$

$$\nabla \cdot \underline{\Sigma}_s = 0 \text{ with B.C. } \underline{\Sigma}_s|_{\partial\Omega^c} \mathbf{n} = \mathbf{0} \text{ and } \underline{\Sigma}_s|_{\partial\omega_t^s} \mathbf{n} = \mathbf{t}_s, \quad (2)$$

where $\mathbf{t}_e = \mathbf{t}_e^S + \mathbf{t}_e^P$ is the total traction stress externally applied to the cell. In the absence of body torques, the local balance of torques insures that $\underline{\Sigma}$ and $\underline{\Sigma}_s$ are symmetric tensors.

- *Conservation of mass in the polymer meshwork.* We denote the polymer meshwork mass density $\rho(\mathbf{x}, t)$ which obeys the following conservation law (Coussy, 2004):

$$\partial_t(\phi\rho) + \nabla \cdot (\phi\rho\mathbf{v}) = R. \quad (3)$$

In the above formula, $\mathbf{v}(\mathbf{x}, t)$ denotes the velocity of the polymer meshwork in the lab frame. The source term $R(\mathbf{x}, t)$ represents the polymer turnover through its polymerization and depolymerization. We complement (3) with no flux boundary conditions and consider that the meshwork cannot flow in and out of the cell at our timescale of interest, where the import and export of proteins is negligible and the dry mass of the cell is almost constant. Therefore, introducing \mathbf{v}_b the velocity of the domain boundary $\partial\omega_t$, we have

$$(\mathbf{v}|_{\partial\omega_t} - \mathbf{v}_b) \cdot \mathbf{n} = 0. \quad (4)$$

Note that (3) can be equivalently written as

$$\frac{d\phi\rho}{dt} = R - \phi\rho\nabla \cdot \mathbf{v}, \quad (5)$$

where $d./dt = \partial_t + \mathbf{v} \cdot \nabla(\cdot)$ denotes the material derivative with respect to the polymer meshwork motion.

- *Conservation of mass in the cytosol.* Next, we assume that the chemical reaction powering the meshwork is happening inside the cytosol. We will simplify the picture by considering a binary reaction where $a(\mathbf{x}, t)$ (ATP concentration) is transformed into $b(\mathbf{x}, t)$ (ADP concentration) inside the cell with a release of energy in the process. The recycling of b into a is performed by catalytic machines (mitochondria) that use nutrients $n(\mathbf{x}, t)$ (such as glucose) that enter the cell and are degraded into products $p(\mathbf{x}, t)$ (such as carbon dioxide) that are expelled out of the cell. Such a recycling happens with a certain stoichiometry whereby one nutrient molecule can recycle ν molecules of b . See Fig. 2 for a schematic of this chemical system. We also consider the monomers

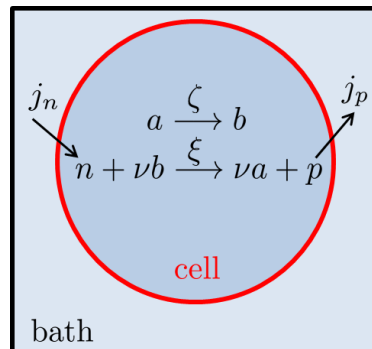


Figure 2: Schematic of the chemical reaction providing the chemical energy necessary to the molecular motors driving the cytoskeleton mechanics.

associated with the polymer meshwork $g(\mathbf{x}, t)$ in solution in the cytosol. As a result, we write the mass balance

laws in the cytosol as

$$\frac{d^f(1-\phi)\rho_f}{dt} = -(1-\phi)\rho_f\nabla\cdot\mathbf{v}_f, \quad (1-\phi)\rho_f\frac{d^f x_g}{dt} = \nabla\cdot\mathbf{J}_g - R, \quad (6)$$

$$(1-\phi)\rho_f\frac{d^f x_a}{dt} = \nabla\cdot\mathbf{J}_a + (1-\phi)\rho_f\left(v\frac{d^f\xi}{dt} - \frac{d^f\zeta}{dt}\right), \quad (1-\phi)\rho_f\frac{d^f x_b}{dt} = \nabla\cdot\mathbf{J}_b - (1-\phi)\rho_f\left(v\frac{d^f\xi}{dt} - \frac{d^f\zeta}{dt}\right), \quad (7)$$

$$(1-\phi)\rho_f\frac{d^f x_n}{dt} = \nabla\cdot\mathbf{J}_n - (1-\phi)\rho_f\frac{d^f\xi}{dt}, \quad (1-\phi)\rho_f\frac{d^f x_p}{dt} = \nabla\cdot\mathbf{J}_p + (1-\phi)\rho_f\frac{d^f\xi}{dt}, \quad (8)$$

where ρ_f is the cytosol mass density that we will assume constant (approximately that of water), $\mathbf{v}_f(\mathbf{x}, t)$ is the velocity field of the cytosol, $d^f./dt = \partial_t + \mathbf{v}_f\cdot\nabla(\cdot)$ denotes the total derivative with respect to the fluid motion, $\zeta(\mathbf{x}, t)$ is the extent of the reaction (also called progress variable or degree of advancement (De Groot and Mazur, 2013)) transforming a into b , $\xi(\mathbf{x}, t)$ the extent of the recycling process and $x_{g,a,b,n,p}(\mathbf{x}, t) = (g, a, b, n, p)/\rho_f$ are the mass fractions of the respective species. These conservation equations are complemented with the boundary conditions

$$(\mathbf{v}_f|_{\partial\omega_t} - \mathbf{v}_b)\cdot\mathbf{n} = 0, \quad \mathbf{J}_{a,b}|_{\partial\omega_t}\cdot\mathbf{n} = 0 \quad \text{and} \quad \mathbf{J}_{n,p}|_{\partial\omega_t}\cdot\mathbf{n} = j_{n,p}. \quad (9)$$

It is therefore assumed for simplicity that water is effectively not flowing in and out the cell at our timescale of interest. Such flows may exist during the fast transient response to osmotic perturbations of the external environment or during the slow growth of the cell during its cycle (Cadart et al., 2019). The system is open at the level of nutrients and products of the recycling of b into a and we denote the incoming flux of n from the bath by j_n and the outgoing flux of p to the bath by j_p . Note that the total mass of monomers and polymer forming the meshwork is constant:

$$\int_{\omega_t} (\phi\rho + (1-\phi)g) d\mathbf{x} = \text{Cst.}$$

Our model neglects the complexity of the actin turnover dynamics which in reality involves a number of intermediate states as well as other interacting proteins (Pollard et al., 2016).

Expression for the dissipation. The rate of external work performed on the total system (cell plus substrate) is

$$\dot{W} = \int_{\partial\omega_t^b} (\mathbf{t}_e^S\cdot\mathbf{v} + \mathbf{t}_e^P\cdot\mathbf{v}_f) ds = \int_{\partial\omega_t^b} (\mathbf{t}_e\cdot\mathbf{v} + \mathbf{t}_e^P\cdot\bar{\mathbf{v}}_f) ds,$$

where $\bar{\mathbf{v}}_f = \mathbf{v}_f - \mathbf{v}$ is the relative velocity of the fluid with respect to the polymer meshwork. Using momentum conservation laws (1)-(2), we obtain that

$$\int_{\partial\omega_t^b} \mathbf{t}_e\cdot\mathbf{v} ds = \int_{\omega_t} \mathbb{\Sigma} : \mathbb{D}(\mathbf{v}) d\mathbf{x} - \int_{\partial\omega_t^s} \mathbf{t}_s\cdot\mathbf{v} ds$$

and

$$0 = \int_{\Omega_t} \mathbb{\Sigma}_s : \mathbb{D}(\mathbf{v}_s) d\mathbf{x} + \int_{\partial\omega_t^s} \mathbf{t}_s\cdot\mathbf{v}_s ds$$

where $:$ is the canonical scalar product on order two tensors, $\mathbf{v}_s(\mathbf{x}, t)$ is the velocity of the substrate and $\mathbb{D}(\cdot)$ is the symmetric part of the related velocity field. With these two relations, we finally obtain that

$$\dot{W} = \int_{\omega_t} (\mathbb{\Sigma} : \mathbb{D}(\mathbf{v}) - \nabla\cdot[(1-\phi)P_f\bar{\mathbf{v}}_f]) d\mathbf{x} + \int_{\omega_t^s} \mathbf{t}_s\cdot\bar{\mathbf{v}}_s ds + \int_{\Omega_t} \mathbb{\Sigma}_s : \mathbb{D}(\mathbf{v}_s) d\mathbf{x}$$

where $\bar{\mathbf{v}}_s = \mathbf{v}_s - \mathbf{v}$.

To compute the rate of change of the free energy, we postulate that

$$F = \int_{\omega_t} [\phi\rho f_{\text{mec}}(\phi\rho, (1-\phi)\rho_f) d\mathbf{x} + (1-\phi)\rho_f f_{\text{chem}}(x_g, x_a, x_b, x_n, x_p) d\mathbf{x} + (1-\phi)\rho_f f_{\text{bio}}(\{\theta_i\}_{i=1..N})] d\mathbf{x} + \int_{\Omega_0} f_{\text{sub}}(\mathbb{E}) d\mathbf{X},$$

where f_{mec} is the mechanical free energy per unit mass of polymer, f_{chem} is the chemical free energy per unit mass of cytosolic solvent, f_{bio} is associated to the complex biological metabolic pathways controlling the recycling of ADP to ATP and f_{sub} is the free energy per unit volume of the visco-elastic substrate (i.e. elastic energy). On the one hand, we assume that f_{mec} depends on the internal variables introduced above that control the level of deformation of the cytoskeleton while f_{chem} depends on the mass fractions of the chemical species in solution in the cytosol. On the other hand, f_{bio} depends on a large ($N \gg 1$) number of internal degrees of freedom $\{\theta_i(\mathbf{x}, t)\}_{i=1..N}$ associated with the recycling process of ADP into ATP involving many complex biochemical and regulatory pathways (such as glycolysis and the Krebs cycle). Finally f_{mec} only depends on the substrate elastic strain \mathbb{E} .

As a simple example, we may specify some classical form of f_{mec} , f_{chem} and f_{sub} while f_{bio} is very complex. Typically, in a mechanically linear theory the dependence of f_{mec} on the polymer and solvent densities is quadratic:

$$f_{\text{mec}} = \frac{K_\rho}{2\bar{\rho}} \left(\frac{\rho\phi - \bar{\rho}}{\bar{\rho}} \right)^2 + \frac{K_{\rho_f}}{2\bar{\rho}_f} \left(\frac{\rho_f(1-\phi) - \bar{\rho}_f}{\bar{\rho}_f} \right)^2 - K_\rho \alpha \frac{\rho\phi\rho_f(1-\phi)}{\bar{\rho}^2\bar{\rho}_f} \quad (10)$$

and

$$f_{\text{chem}} = \sum_{i=g,a,b,n,p} \frac{R_i}{2} \left(\frac{x_i - \bar{x}_i}{\bar{x}_i} \right)^2. \quad (11)$$

In the above expressions, K_ρ and K_{ρ_f} are compressibility moduli, $\bar{\rho}$ and $\bar{\rho}_f$ equilibrium densities, α a Biot coefficient characterizing the mechanical coupling between the cytoskeletal and cytosol phases and $\bar{x}_{g,a,b,n,p}$ equilibrium mass fractions. The coefficients

$$R_i = \frac{k_B T N_A}{m_i}$$

are the specific gas constant of each specie (k_B is the Boltzmann constant, N_A the Avogadro number and m_i the molar mass of the i^{th} specie). In the same way, a classical quadratic form of the substrate free energy per unit volume is

$$f_{\text{sub}} = \frac{3K_s - 2G_s}{6} \text{tr}(\mathbb{E})^2 + G_s \mathbb{E} : \mathbb{E}$$

which corresponds to a Saint-Venant Kirchhoff material with bulk modulus K_s and shear modulus G_s . However, these expressions are only examples to fix ideas and the rest of the theory does not rely on this specific choice.

We can directly compute the rate of change of free energy as

$$\dot{F} = \int_{\omega_t} \left(R f_{\text{mec}} + \phi \rho \frac{d f_{\text{mec}}}{dt} + (1-\phi) \rho_f \frac{d f_{\text{chem}}}{dt} + (1-\phi) \rho_f \frac{d f_{\text{bio}}}{dt} \right) d\mathbf{x} + \int_{\Omega_t} \frac{1}{\det \mathbb{F}} \frac{d f_{\text{sub}}}{dt} d\mathbf{x},$$

where $d^s./dt = \partial_t + \mathbf{v}_s \cdot \nabla(\cdot)$ is the material derivative in the substrate. We additionally write that the rate of free energy input and output in the system is locally proportional to the rate of delivery and removal of n and p (since the system is closed for all other species),

$$\dot{F}_e = \int_{\omega_t} (j_n \mu_n^0 + j_p \mu_p^0) ds = \int_{\omega_t} (\mu_n^0 \nabla \cdot \mathbf{J}_n + \mu_p^0 \nabla \cdot \mathbf{J}_p) ds.$$

Here we have introduced the constant free energies per unit mass $\mu_{n,p}^0$ of n and p when they are brought in (j_n is positive) and removed (j_p is negative) from the system. This is similar to considering the grand canonical ensemble with a bath that maintains fixed chemical potentials (in other words, a chemostat). Using the chain rule, we obtain

$$\begin{aligned} \frac{d f_{\text{mec}}}{dt} &= \frac{\partial f_{\text{mec}}}{\partial \phi \rho} \frac{d \phi \rho}{dt} + \frac{\partial f_{\text{mec}}}{\partial (1-\phi) \rho_f} \frac{d (1-\phi) \rho_f}{dt}, \quad \frac{d f_{\text{chem}}}{dt} = \sum_{i=g,a,b,n,p} \frac{\partial f_{\text{chem}}}{\partial x_i} \frac{d x_i}{dt}, \\ \frac{d f_{\text{bio}}}{dt} &= \sum_{i=1..N} \frac{\partial f_{\text{bio}}}{\partial \theta_i} \frac{d \theta_i}{dt} \quad \text{and} \quad \frac{d f_{\text{sub}}}{dt} = \frac{\partial f_{\text{sub}}}{\partial \mathbb{E}} : \frac{d \mathbb{E}}{dt}. \end{aligned}$$

Therefore, using the conservation laws (5)-(8), we can express dissipation as the sum of products of generalized forces by generalized fluxes

$$\begin{aligned}
\mathcal{D} = & \int_{\omega_i} \left((\Sigma + \phi P \mathbb{I} + (1 - \phi) P_f \mathbb{I}) : \mathbb{D} - (1 - \phi) \bar{\mathbf{v}}_f \nabla P_f + R(\mu_g - \mu) + \sum_{i=g,a,b,n,p} \mathbf{J}_i \nabla \mu_i \right. \\
& + (1 - \phi) \rho_f \frac{d^f \xi}{dt} (\Delta \mu_{np} - \nu \Delta \mu_{ab}) + (1 - \phi) \rho_f \frac{d^f \zeta}{dt} \Delta \mu_{ab} \\
& - \sum_{i=1..N} (1 - \phi) \rho_f \frac{d^f \theta_i}{dt} \mu_{\theta_i} \Big) d\mathbf{x} + \int_{\partial \omega_i} (j_n(\mu_n^0 - \mu_n |_{\partial \omega_i}) + j_p(\mu_p^0 - \mu_p |_{\partial \omega_i})) ds \\
& + \int_{\omega_i^s} \mathbf{t}_s \cdot \bar{\mathbf{v}}_s ds + \int_{\Omega_i} \left(\mathbb{F}^{-1} \Sigma_s \mathbb{F}^{-T} - \frac{1}{\det \mathbb{F}} \frac{\partial f_{\text{sub}}}{\partial \mathbb{E}} \right) : \frac{d^s \mathbb{E}}{dt} d\mathbf{x} \geq 0.
\end{aligned} \tag{12}$$

In (12), $P = \phi \rho^2 \partial_{\phi \rho} f_{\text{mec}}$ is the thermodynamic pressure in the polymer meshwork, $P_f = \phi \rho \rho_f \partial_{(1-\phi)\rho_f} f_{\text{mec}}$, is the hydrostatic pressure in the permeating fluid, $\mu = f_{\text{mec}} + P/\rho$ is the Gibbs chemical potential of the polymer, $\mu_{g,a,b,n,p} = \partial_{x_{g,a,b,n,p}} f_{\text{chem}}$ are the chemical potentials of the monomers, ADP, ATP nutrients and products in solution in the cytosol. We define $\Delta \mu_{np} = \mu_n - \mu_p$ and $\Delta \mu_{ab} = \mu_a - \mu_b$. Finally the $\mu_{\theta_i} = \partial_{\theta_i} f_{\text{bio}}$ are the chemical potentials of the biochemical degrees of freedom that fully describe the biochemical processes regulating the recycling of ADP to ATP. The generalized force-flux pairs entering in the dissipation and the conservation laws associated to the generalized fluxes can be summarized in Table 1.

<i>generalized force</i>	<i>generalized flux</i>	<i>conservation law</i>
\mathbb{D}	$\Sigma + \phi P \mathbb{I} + (1 - \phi) P_f \mathbb{I}$	cell momentum balance (1)
$-\nabla P_f$	$(1 - \phi) \bar{\mathbf{v}}_f$	fluid conservation (6) ₁
$\mu_g - \mu$	R	polymer conservation (3)
$\nabla \mu_i$	\mathbf{J}_i	solutes conservation (6) ₂ – (7) – (8)
$\Delta \mu_{np} - \nu \Delta \mu_{ab}$	$(1 - \phi) \rho_f d^f \xi / dt$	metabolites conservation (7) – (8)
$\Delta \mu_{ab}$	$(1 - \phi) \rho_f d^f \zeta / dt$	metabolites conservation (7)
$-\mu_{\theta_i}$	$(1 - \phi) \rho_f d^f \theta_i / dt$	recycling processes
$\mu_{n,p}^0 - \mu_{n,p}$	$j_{n,p} _{\partial \omega_i}$	nutrients and products fluxes (9) ₃
$\bar{\mathbf{v}}_s$	\mathbf{t}_s	cell-substrate traction forces (1) – (2)
$d^s \mathbb{E} / dt$	$\mathbb{F}^{-1} \Sigma_s \mathbb{F}^{-T} - \det \mathbb{F}^{-1} \partial f_{\text{sub}} / \partial \mathbb{E}$	substrate momentum balance (2)

Table 1: Force-flux pairs entering in the dissipation expression (12). The fluxes are associated to their specific conservation laws.

Generalized forces-fluxes relations. Close to thermodynamic equilibrium, the generalized fluxes entering in the dissipation can be written as a linear combination (with some symmetries on the kinetic coefficients) of the generalized forces according to Onsager's principle (De Groot and Mazur, 2013). In particular, we can write the constitutive relations:

$$\begin{aligned}
\Sigma &= -\phi P \mathbb{I} - (1 - \phi) P_f \mathbb{I} + \eta \mathbb{D} + \chi_{\Sigma a} \Delta \mu_{ab} \mathbb{I}, \quad (1 - \phi) \bar{\mathbf{v}}_f = -\frac{\kappa}{\eta_f} \nabla P_f \text{ and } R = k_\rho (\mu_g - \mu) \\
\mathbf{J}_{g,a,b,n,p} &= M_{g,a,b,n,p} \nabla \mu_{g,a,b,n,p} \text{ and } j_{n,p} = L_{n,p} (\mu_{n,p}^0 - \mu_{n,p} |_{\partial \omega_i}) \\
\rho_f (1 - \phi) \frac{d^f \zeta}{dt} &= \chi_{a \Sigma} \nabla \cdot \mathbf{v} + k_a \Delta \mu_{ab} \\
\rho_f (1 - \phi) \frac{d^f \xi}{dt} &= k_n (\Delta \mu_{np} - \nu \Delta \mu_{ab}) - \sum_{i=1..N} \lambda_{ni} \mu_{\theta_i}, \\
\forall i = 1..N, \rho_f (1 - \phi) \frac{d^f \theta_i}{dt} &= -\lambda_{ii} \mu_{\theta_i} + \lambda_{in} (\Delta \mu_{np} - \nu \Delta \mu_{ab}), \\
\mathbf{t}_s &= \tilde{\lambda} \bar{\mathbf{v}}_s \text{ and } \Sigma_s = \mathbb{F} \left(\frac{1}{\det \mathbb{F}} \frac{\partial f_{\text{sub}}}{\partial \mathbb{E}} + \eta_s \frac{d^s \mathbb{E}}{dt} \right) \mathbb{F}^T.
\end{aligned} \tag{13}$$

In (13), we have neglected a certain number of cross-couplings to only retain:

1. The active stress driven by the chemical reaction transforming a into b and the corresponding cross term in the equation giving the dynamics of ζ . Because the strain rate is odd under time reversal while $\Delta\mu_{ab}$ is even, we have $\chi_{\Sigma a} = -\chi_{a\Sigma}$ (Kruse et al., 2005). The active stress is isotropic here but it can be given deviatoric components by involving in the free energy a polarity field as in more general liquid crystal theories (Kruse et al., 2005). We also neglect for sake of simplicity the fact that the growth properties of the polymer meshwork can be actively controlled by the ATP hydrolysis which could be easily accounted for by introducing a cross-coupling term between R and $\Delta\mu_{ab}$ (and its symmetric counterpart).
2. The regulating action of the micro-variables θ_i on the kinetics of the recycling process of ADP to ATP. Therefore the θ_i may be understood as all the molecular degrees of freedom involved in the running of mitochondria. As the sign reversal signature is the same for all coupled variables in this case, we have the symmetry relations and $\lambda_{ni} = \lambda_{in}$.

In (13), we have also neglected any type of material anisotropy and η denotes the viscosity of the polymer meshwork, $\eta_f (\ll \eta$ in practice) is the viscosity of the permeating fluid, κ is the permeability (in $[m^2]$) of the polymer meshwork, k_p is the rate of renewal of the network, $M_{g,a,b,n,p}$ are the Fickian mobilities of the various species in solution, $L_{n,p}$ are the permeabilities of the cell membrane to the nutrients and the products, k_a is the rate of the chemical reaction transforming ATP into ADP and k_n the rate of turnover of nutrients into products. Finally, $\tilde{\lambda}$ is a friction coefficient of the cell with its substrate and η_s is the substrate viscosity. For a purely elastic substrate, we recover the general relation giving the Cauchy stress as a function of the elastic energy $\Sigma_s = \frac{1}{\det \mathbb{F}} \mathbb{F} \frac{\partial f_{\text{sub}}}{\partial \mathbb{E}} \mathbb{F}^T$ while for small deformations of substrate, we obtain the usual linear relation $\Sigma_s = \frac{\partial f_{\text{sub}}}{\partial \mathbb{E}} + \eta_s \frac{d^s \mathbb{E}}{dt}$.

3. Energy homeostasis

Combining the last two equations of (13) to eliminate μ_{θ_i} , we obtain the kinetics of the metabolic recycling of ADP into ATP:

$$\rho_f(1 - \phi) \frac{d^f \xi}{dt} = (k_n - \bar{\lambda}_n) (\Delta\mu_{np} - v\Delta\mu_{ab}) + \sum_{i=1..N} \frac{\lambda_{ni}}{\lambda_{ii}} \rho_f(1 - \phi) \frac{d^f \theta_i}{dt} \text{ where, } \bar{\lambda}_n = \sum_{i=1..N} \frac{\lambda_{ni}^2}{\lambda_{ii}}$$

At this stage, we make the strong modeling assumption that, because the $\mu_{\theta_i} (\{\theta_i\}_{i=1..N})$ are complex coupled functions, the large system of equations ruling the dynamics of the internal degrees of freedom θ_i is also complex and, to effectively describe the collective θ_i dynamic, we suppose that these variables are independent and identically distributed stochastic processes. In such a case, according to the central limit theorem,

$$X(\mathbf{x}, t) = \rho_f(1 - \phi) \sum_{i=1..N} \frac{\lambda_{ni}}{\lambda_{ii}} \theta_i(\mathbf{x}, t)$$

converges to a biased Brownian motion characterized by a certain mean X_0 and variance Θ . The mean is irrelevant here as the θ_i only enter the problem under a time derivative. This constitutive assumption that represents the recycling of metabolites as an equilibrium system is of course questionable for many systems as, for instance, chemical reactions are known to produce coloured rather than white noise (Sekimoto, 2010). But this simple closure provides a noisy chemical recycling dynamics

$$\rho_f(1 - \phi) \frac{d^f \xi}{dt} = \bar{k}_n (\Delta\mu_{np} - v\Delta\mu_{ab}) + \frac{d^f X}{dt},$$

where

$$\bar{k}_n = k_n - \bar{\lambda}_n.$$

Thus, the stochasticity of the energy delivery entails a stochastic behaviour of x_a and x_b resulting in a stochastic mechanical system through the active stress. This in particular implies that cell motility, which is driven by its cytoskeleton, is controlled by the recycling of ATP as we shall demonstrate in the following section. Correlation between fluctuations of cell shape changes and ATP concentration have been experimentally demonstrated by Suzuki et al. (2015).

Although we have reduced the θ_i biochemical variables involved in the recycling of ADP to ATP to a single effective parameter Θ , we have not specified yet how these variables collectively regulate the energy recycling process. To do so, we first define the chemo-mechanical cell free-energy as

$$F_{cm} = F_{mec} + F_{chem} = \int_{\omega_t} \phi \rho f_{mec}(\phi \rho, (1 - \phi) \rho_f) d\mathbf{x} + \int_{\omega_t} (1 - \phi) \rho_f f_{chem}(x_g, x_a, x_b, x_n, x_p) d\mathbf{x}.$$

The rate of change of F_{mec} is associated with the energetic cost for the cell to perform its mechanical tasks like changing its shape or moving its center of mass (Recho et al., 2014). Following the idea presented in (Shishvan et al., 2018; Buskermolen et al., 2019) we postulate that changes of F_{mec} are compensated by changes of F_{chem} such that the total chemo-mechanical free energy F_{cm} is fixed independently of the external mechanical loading. This is a constitutive assumption that we associate with the biological idea of cell energy homeostasis. In other words, the cell machinery functions to maintain at a constant level the energy resource that can be employed by the cytoskeleton. Thus, denoting by $\mathbb{E}(\cdot)$ the ensemble averaging over the noise fluctuations, the amplitude of the fluctuations Θ is set by the non local (in both space and time) constraint:

$$\lim_{\tilde{t} \rightarrow \infty} \frac{1}{\tilde{t}} \int_0^{\tilde{t}} \mathbb{E}(F_{cm}) dt = F_0, \quad (14)$$

where F_0 is a constant average value over both time and stochastic fluctuations of the chemo-mechanical free energy, which is evaluated from that of a suspended cell (i.e. in the absence of geometrical confinement or external force).

The full model is therefore composed of the mass and momentum conservation laws in which the general constitutive relations of the active medium are given by the Forces-fluxes Onsager relations (13). These relations are simplified by assuming that the large number of internal metabolic degrees of freedom that characterize the recycling of the energy delivery process to the cytoskeleton can be treated as an equilibrium reservoir that controls the global free energy of the cell to a target value by the homeostatic constraint (14). Because the active stress entering in the Onsager relations stems from a dissipative coupling between cytoskeleton mechanics and ATP hydrolysis through $\chi_{\Sigma a}$, the active stress becomes a stochastic variable that is controlled by the metabolism. Reciprocally, the rate of recycling of the energy delivery to the cytoskeleton is influenced by cell mechanics in general, and by the mechanical environment of the cell in particular.

4. Example: an active stochastic segment

Rather than giving a general discussion of the theoretical framework developed above, we illustrate and explain its implications in the simple case of a one-dimensional infinitely thin segment of active gel crawling along a straight rigid track. Our aim is to spell out the general coupling discussed above in this special case and show how it can help to understand the stochastic nature of cell motility. In this situation $\omega_t = [L_-(t), L_+(t)]$ where $L_- < L_+$ denote the positions of the cell fronts. To simplify the formulation of the problem, we introduce the traveling coordinate $y = x - L_- \in [0, L]$ where $L = L_+ - L_-$ is the gel length. In this new coordinate system $\partial_x = \partial_y$, and $\partial_t|_y = \partial_t|_x + \dot{L}_- \partial_x|_x$, where the superimposed dot denotes the time derivative of the front position.

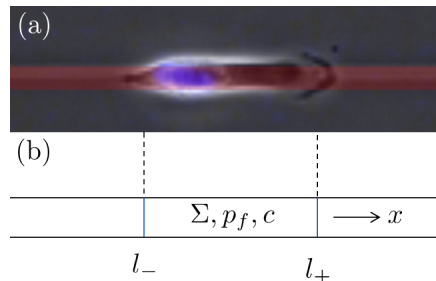


Figure 3: (a) Human renal adenocarcinoma migrating on a fibronectin coated track from Maiuri et al. (2012). (b) Scheme of the crawling active gel segment.

4.1. Mechanics of the active gel segment

As the track is considered to be infinitely stiff, the substrate velocity vanishes ($v_s = 0$) and we obtain from the last line of (13) that $t_s = -\tilde{\lambda}v$. In the context of a thin film approximation (the cell height $h \ll L$), this friction results in a body force $-\lambda v$ where the rescaled friction coefficient is $\lambda = \tilde{\lambda}/h$. See Roux et al. (2016) for details. From (1), the global force balance therefore reads

$$\partial_y \Sigma = \lambda v. \quad (15)$$

As we do not consider any additional external force, (15) is associated with the boundary conditions:

$$\Sigma|_{0,L} = 0. \quad (16)$$

The first relation of (13) provides the constitutive behaviour of the gel

$$\Sigma = -\phi P - (1 - \phi)P_f + \eta \partial_y v + \chi_{\Sigma a} \Delta \mu_{ab}. \quad (17)$$

To specify the pressure terms P and P_f , we consider the free energy expression (10) and obtain

$$P = K_\rho \phi \frac{\rho^2}{\bar{\rho}^2} \left[\frac{\rho \phi - \bar{\rho}}{\bar{\rho}} - \alpha \frac{\rho_f (1 - \phi)}{\bar{\rho}_f} \right] \text{ and } P_f = \phi \frac{\rho \rho_f}{\bar{\rho}_f^2} \left[K_{\rho_f} \frac{\rho_f (1 - \phi) - \bar{\rho}_f}{\bar{\rho}_f} - \alpha K_\rho \frac{\bar{\rho}_f \rho \phi}{\bar{\rho}^2} \right].$$

Next, we make the realistic assumptions that the polymer meshwork is highly compressible while the volume fraction is fixed and hence consider the limit where $K_\rho = 0$, $K_{\rho_f} = \infty$ and $\rho_f (1 - \phi) = \bar{\rho}_f$ while the product $K_{\rho_f} (\rho_f (1 - \phi) - \bar{\rho}_f)$ remains finite. These assumptions entail that the volume fraction is fixed $\phi = 1 - \bar{\rho}_f / \rho_f$ and P_f is a Lagrange multiplier determined by the solvent mass conservation relation (6)₁ which reduces to:

$$\partial_y v_f = 0.$$

Hence, using the boundary conditions (9) the fluid velocity is a constant equal to the common velocity of the moving fronts $v_f = V = \dot{L}_- = \dot{L}_+$ where $V(t)$ denotes the common front velocity.

Combining this simple relation with the Darcy law obtained from (13), we derive the hydrostatic pressure field:

$$(1 - \phi)(V - v) = -\frac{\kappa}{\eta_f} \partial_y P_f. \quad (18)$$

From the boundary conditions associated with the absence of flow of polymer outside the cell membrane (4), we have

$$v|_{0,L} = V \text{ so that } \partial_y P_f|_{0,L} = 0.$$

Another useful consequence of the infinite compressibility of the polymer meshwork and fixed volume fraction is that the mechanical free energy reduces to zero

$$f_{\text{mec}} = 0. \quad (19)$$

Note that as the constitutive behaviour (17) no longer involves P , the mass balance equation for the polymer (3)₁ uncouples from the mechanical problem and the meshwork density ρ can be reconstructed afterwards (in tandem with the concentration of monomers g) when the velocity field v is determined (see for instance (Recho et al., 2013, 2015)). For simplicity, we suppose that ρ is fixed at a constant corresponding to the local chemical equilibrium between the polymerization of the meshwork and its depolymerization. More specifically, plugging the assumption of constant ρ into (3)₁ with the turnover rate R given by (13), we obtain

$$k_\rho^{-1} \phi \rho \partial_y v = \mu_g - \mu$$

which, if the rate of turnover k_ρ is much larger than the rate of transport, reduces to $\mu(\rho) = \mu_g(\bar{x}_g)$. This last relation fixes the value of ρ at a constant if the diffusion of g is large enough such that its concentration is homogeneous in the whole cell: $x_g = \bar{x}_g$.

With these simplifying but realistic assumptions, the mechanical problem describing the cytoskeleton can be formulated in the compact form

$$\begin{cases} -\frac{\eta}{\lambda}\partial_{yy}\Sigma + \Sigma = -(1-\phi)P_f + \chi_{\Sigma a}\Delta\mu_{ab} \\ \partial_{yy}\left[\frac{\Delta\kappa}{\eta_f}P_f - (1-\phi)\Sigma\right] = 0. \end{cases} \quad (20)$$

The boundary conditions associated to (20) are

$$\Sigma|_{0,L} = 0 \text{ and } \partial_y P_f|_{0,L} = 0. \quad (21)$$

Once (20)-(21) is solved, the cell front dynamics can be computed from the integration of (18) over the whole segment:

$$(1-\phi)V(t)L = -\frac{\kappa}{\eta_f}\left[P_f(L,t) - P_f(0,t)\right]. \quad (22)$$

When $\Delta\mu_{ab}$ is fixed, (20)-(21) reduces to an isotropic active gel model similar to that studied in Jülicher et al. (2007). However, the ingredient of the permeation of the cytosol in the cytoskeleton (Alt and Dembo, 1999; Callan-Jones and Voituriez, 2013; Kimpton et al., 2015) has been added to this classical model. The model equations (20) describe a non-polarized cell. Several mechanisms leading to a spontaneous cell mechanical polarization have been discussed in the literature (See for instance Callan-Jones and Voituriez (2013); Recho et al. (2013); Blanch-Mercader and Casademunt (2013); Tjhung et al. (2012); Edelstein-Keshet et al. (2013); Giomi and DeSimone (2014)) and could be added to this framework. We have deliberately left this important effect aside to focus on the coupling of mechanics with metabolism and the ensuing stochastic nature of the cell motion. To do so, system (20) is now coupled with a paradigmatic model of the cell metabolism that dynamically sets $\Delta\mu_{ab}$. This coupling introduces stochasticity in the deterministic mechanical model as detailed below.

4.2. Dynamics of the energy delivery

From the Onsager relations (13) and the mass balance equations (7)-(8) of the solute chemical species a, b, n and p , we obtain

$$\begin{aligned} \rho_f(1-\phi)\partial_t x_a &= M_a\partial_{yy}\mu_a + \left[v\bar{k}_n(\Delta\mu_{np} - v\Delta\mu_{ab}) + v\partial_t X + \chi_{\Sigma a}\partial_y v - k_a\Delta\mu_{ab} \right] \\ \rho_f(1-\phi)\partial_t x_b &= M_b\partial_{yy}\mu_b - \left[v\bar{k}_n(\Delta\mu_{np} - v\Delta\mu_{ab}) + v\partial_t X + \chi_{\Sigma a}\partial_y v - k_a\Delta\mu_{ab} \right] \\ \rho_f(1-\phi)\partial_t x_n &= M_n\partial_{yy}\mu_n - \left[\bar{k}_n(\Delta\mu_{np} - v\Delta\mu_{ab}) + \partial_t X \right] \\ \rho_f(1-\phi)\partial_t x_p &= M_p\partial_{yy}\mu_p + \left[\bar{k}_n(\Delta\mu_{np} - v\Delta\mu_{ab}) + \partial_t X \right]. \end{aligned} \quad (23)$$

Using some technical assumptions that rely on the fast diffusion of these chemical species and that are explained in detail in Appendix A, we can simplify (23) to the single partial differential equation

$$\partial_t\Delta\mu_{ab} = D_{ab}\partial_{yy}\Delta\mu_{ab} + \frac{2\kappa\chi_{\Sigma a}}{\alpha_{ab}(1-\phi)\eta_f}\partial_{yy}P_f - \frac{2k_{na}}{\alpha_{ab}}\Delta\mu_{ab} + \frac{2v\bar{k}_n}{\alpha_{ab}}\Delta\mu_{np}^0 + \frac{2v}{\alpha_{ab}}\Gamma, \quad (24)$$

which encapsulates the kinetics of the metabolism that provides energy to the molecular motors actuating the active gel. In (24), D_{ab} (estimated in Table 2) is an effective diffusion coefficient of the metabolites in the cytosol and $\Gamma(y, t) = \partial_t X(y, t)$ is a Gaussian process satisfying

$$\mathbb{E}(\Gamma(y, t)) = 0 \text{ and } \mathbb{E}(\Gamma(y, t)\Gamma(y', t')) = 2\Theta\min(y, y')\delta(t - t').$$

Note that the physical dimension of Θ is thus given by $[\Theta] = \text{kg}^2\text{m}^{-7}\text{s}^{-1}$.

Mechanics and metabolism are coupled by the Onsager coefficient $\chi_{\Sigma a}$ which enters in both (20) and (24). In the absence of metabolic noise in the system, $\Gamma = 0$ and the solution of the problem is trivial:

$$\Delta\mu_{ab} = \Delta\mu_{ab}^0 = v\frac{\bar{k}_n}{k_{na}}\Delta\mu_{np}^0. \quad (25)$$

This leads to an homogeneous distribution of stresses within the active gel segment:

$$\Sigma = \Sigma^0 = 0 \text{ and } P_f = P_f^0 = \chi_{\Sigma a}\Delta\mu_{ab}^0/(1-\phi).$$

name	symbol	typical value
cytoskeleton viscosity	η	10^3 Pa s (Jülicher et al., 2007; Rubinstein et al., 2009)
cytosol viscosity	η_f	2×10^{-3} Pa s (Moeendarbary et al., 2013)
cytoskeleton permeability	κ	2×10^{-16} m ² (Moeendarbary et al., 2013)
solid volume fraction	ϕ	0.25 (Moeendarbary et al., 2013)
energy production per unit mass	$\Delta\mu_{ab}^0$	10^5 J.kg ⁻¹ (Jülicher et al., 2007)
contractility	$\chi_{\Sigma a}\Delta\mu_{ab}^0$	10^3 Pa (Jülicher et al., 2007; Rubinstein et al., 2009)
viscous friction coefficient	λ	10^{15} Pa s m ⁻² (Jülicher et al., 2007; Barnhart et al., 2011)
cell length	L	10^{-5} m
energy conversion coefficient	α_{ab}	10^{-5} kg ² m ⁻³ J ⁻¹ [see Appendix A]
diffusion of ATP/ADP	D_{ab}	10^{-12} m ² s ⁻¹ [see Appendix A]
number of ATP recycled with one nutrient	ν	30 (Alberts et al., 2002)
rate of the ATP to ADP reaction in motors	k_a/α_{ab}	25 s ⁻¹ (Howard et al., 2001)
rate of the ATP recycling	\bar{k}_n/α_{np}	0.01 s ⁻¹ (Skog et al., 1982)
effective rate (see (A.2))	k_{na}/α_{ab}	25 s ⁻¹

Table 2: Estimates of material and kinetic coefficients entering in the chemo-mechanical model. It is however important to keep in mind that some of these biophysical parameters (such as cytoskeleton viscosity or the viscous friction coefficient Barnhart et al. (2011) for instance) can vary over several orders of magnitudes depending on the cell type.

In the presence of metabolic noise, we write $\Delta\mu_{ab} = \Delta\mu_{ab}^0 + \delta\mu_{ab}$, $\Sigma = \Sigma^0 + \delta\Sigma$ and $P_f = P_f^0 + \delta P_f$ where, given the linearity of equation (24), $\delta\mu_{ab}$ is a stochastic variable with a zero mean ($\mathbb{E}(\delta\mu_{ab}) = 0$) whose amplitude is set by the noise amplitude. Therefore, to close the problem, it remains to apply the energetic constraint that sets the value of Θ . In the framework of the active segment, the energy homeostasis assumption (14) reads:

$$\lim_{\tilde{t} \rightarrow \infty} \frac{1}{L\tilde{t}} \int_0^{\tilde{t}} \int_0^L \mathbb{E}(\delta\mu_{ab}^2) dy dt = \mu_0^2, \quad (26)$$

where μ_0^2 is a constant explicitly related to F_0 (See Appendix A).

4.3. Solution of the chemo-mechanical problem

Combining the mechanical problem (20) and (21) and the kinetics of the metabolism controlling the active stress (24), we obtain the coupled chemo-mechanical stochastic problem:

$$\begin{cases} -\frac{\eta}{\lambda} \partial_{yy} \delta\Sigma + \delta\Sigma = -(1-\phi) \delta P_f + \chi_{\Sigma a} \delta\mu_{ab} \\ \partial_{yy} \left[\frac{\lambda\kappa}{\eta_f} \delta P_f - (1-\phi) \delta\Sigma \right] = 0 \\ \partial_t \delta\mu_{ab} = D_{ab} \partial_{yy} \delta\mu_{ab} + \frac{2\kappa\chi_{\Sigma a}}{\alpha_{ab}(1-\phi)\eta_f} \partial_{yy} \delta P_f - \frac{2k_{na}}{\alpha_{ab}} \delta\mu_{ab} + \frac{2\nu}{\alpha_{ab}} \Gamma \end{cases} \quad (27)$$

with boundary conditions

$$\delta\Sigma|_{0,L} = 0, \partial_y \delta P_f|_{0,L} = 0 \text{ and } \partial_y \delta\mu_{ab}|_{0,L} = 0. \quad (28)$$

The parameters entering in (27)-(28) can be estimated based on various experiments, see Table 2.

To solve the above linear but non-local problem, we first consider the first two equations in (27) with their associated boundary conditions to obtain the following expression

$$\partial_{yy} P_f[\delta\mu(y, t)] = \frac{\lambda\chi_{\Sigma a} \left(\frac{\eta\Lambda^2}{\lambda} - 1 \right)}{\eta(1-\phi)} \left(\frac{\Lambda \left(\int_y^L \psi(u, y) \delta\mu(u, t) du + \int_0^y \psi(y, u) \delta\mu(u, t) du \right)}{L\Lambda \left(\frac{\eta\Lambda^2}{\lambda} - 1 \right) \sinh(L\Lambda) + 4 \sinh^2 \left(\frac{L\Lambda}{2} \right)} - \delta\mu(y, t) \right),$$

where the interaction kernel reads

$$\psi(y, u) = L\Lambda \left(\frac{\eta\Lambda^2}{\lambda} - 1 \right) \cosh(u\Lambda) \cosh(\Lambda(L-y)) + 2 \sinh \left(\frac{L\Lambda}{2} \right) \cosh \left(\Lambda \left(\frac{L}{2} + u - y \right) \right).$$

This kernel is obtained using the standard method of the variation of constants for a second order problem. In the expressions above, we have introduced the hydrodynamic wavelength

$$\Lambda = \sqrt{\frac{\kappa\lambda + \eta_f(1 - \phi)^2}{\eta\kappa}},$$

a generalization of the quantity introduced in Jülicher et al. (2007). Next, we write

$$\delta\mu(y, t) = \sum_{k=0}^{\infty} \delta\mu_k(t)w_k(y) \text{ with } \delta\mu_k(t) = \int_0^L \delta\mu(y, t)w_k(y)dy$$

and

$$\delta\Gamma(y, t) = \sum_{k=0}^{\infty} \Gamma_k(t)w_k(y) \text{ with } \Gamma_k(t) = \int_0^L \Gamma(y, t)w_k(y)dy$$

to project the last equation of (27) on the Hilbert-Schmidt basis

$$w_k(y) = \sqrt{\frac{2}{L}} \cos\left(\frac{k\pi}{L}y\right).$$

After an exponentially decaying transient, the steady state modes of $\delta\mu$ are given by the relations (See Appendix B.)

$$\forall k \geq 0, \begin{cases} \delta\mu_{2k}(t) = \frac{2}{\alpha_{ab}} \int_0^t e^{d_{2k}(t-u)} \Gamma_{2k}(u) du \\ \delta\mu_{2k+1}(t) = \frac{2}{\alpha_{ab}} \int_0^t e^{d_{2k+1}(t-u)} \Gamma_{2k+1}(u) du + \frac{2}{\alpha_{ab}s} \int_0^t e^{d_{2k+1}(t-u)} (e^{s(t-u)} - 1) \beta_{2k+1} \sum_{l=0}^{\infty} \gamma_{2l+1} \Gamma_{2l+1}(u) du, \end{cases} \quad (29)$$

where the three sequences entering in (29) are given by:

$$d_k = -\left(\frac{k^2\pi^2}{\tau_d} + \frac{2}{\tau_r} + \frac{2\pi^2k^2}{\tau_a(\pi^2k^2 + f^2)}\right), \gamma_k = -\frac{4\sqrt{2/L}f^2 \operatorname{sech}(f/2)}{\tau_a(\pi^2k^2 + f^2)(pf - f + 2 \tanh(f/2))} \text{ and } \beta_k = \frac{2\sqrt{2L}f \cosh(f/2)}{\pi^2k^2 + f^2}$$

and the scalar s reads:

$$s = \frac{(f - \sinh(f))\operatorname{sech}^2(f/2)}{\tau_a(fp - f + 2 \tanh(f/2))}.$$

In the above expression, we have introduced the characteristic timescales representing the diffusion time, the reaction time and a transport time mediated by the molecular motors

$$\tau_d = \frac{L^2}{D_{ab}}, \tau_r = \frac{\alpha_{ab}}{k_{na}} \text{ and } \tau_a = \frac{\eta\alpha_{ab}}{\chi_{\Sigma a}^2}$$

and two non-dimensional parameters :

$$f = \Lambda L = \frac{L}{l_0} \left(Q_\lambda + \frac{1}{Q_\eta}\right)^{1/2} \text{ and } p = \frac{\eta\Lambda^2}{\lambda} = 1 + \frac{1}{Q_\lambda Q_\eta}.$$

For a more transparent physical interpretation, we have also expressed f and p as a function of $l_0 = \sqrt{\kappa}/(1 - \phi)$ the characteristic permeation length scale, $Q_\eta = \eta/\eta_f$ the non-dimensional ratio of the cytoskeleton to cytosol viscosity and $Q_\lambda = \lambda\kappa/(\eta(1 - \phi)^2)$ which is another non-dimensional parameter representing the external friction due to the environment divided by the internal friction of the cytoskeleton in the cytosol. The cell environment properties are therefore all encapsulated in this last parameter Q_λ . Our simple model of non-polarizable cell motility on a one dimensional track essentially depends on a few non-dimensional parameters only, namely Q_λ , Q_η , two independent ratios of the three characteristic timescales τ_d , τ_r and τ_a and the ratio of the two lengthscales L/l_0 .

Finally, we use the relations (29) to set Θ according to the global energy homeostasis constraint (26). Using the noise statistics property

$$\mathbb{E}(\Gamma_k(t)\Gamma_l(t')) = 2\Theta \int_0^L \int_0^L \min(y, y')\delta(t - t')w_k(y)w_l(y')dydy' = 2\Theta\delta(t - t')\delta(l - k) \begin{cases} \frac{2L^2}{3} & \text{if } k = 0 \\ \frac{L^2}{k^2\pi^2} & \text{if } k \geq 1 \end{cases}, \quad (30)$$

we obtain the relation setting Θ as a function of the constant value μ_0^2 ,

$$\mu_0^2 = \lim_{\tilde{t} \rightarrow \infty} \frac{1}{L\tilde{t}} \int_0^{\tilde{t}} \sum_{k=0}^{\infty} \mathbb{E}(\delta\mu_k^2) dt = \frac{\Theta L \tau_r}{\alpha_{ab}^2} \left(\frac{4}{3} - \sum_{k=1}^{\infty} \frac{1}{\tau_r (2\pi k)^2 d_{2k}} - 4 \sum_{k=0}^{\infty} \frac{s^2 - 2(s + d_{2k+1})\beta_{2k+1}\gamma_{2k+1} + 3sd_{2k+1} + 2d_{2k+1}^2 + \bar{s}\beta_{2k+1}^2}{\tau_r(\pi(2k+1))^2 d_{2k+1}(s + d_{2k+1})(s + 2d_{2k+1})} \right), \quad (31)$$

where

$$\bar{s} = \sum_{k=0}^{\infty} \gamma_{2k+1}^2.$$

As a consequence, depending on the mechanical properties of the environment, the biochemical regulation of the recharging of ADP into ATP is influenced to comply with the homeostatic energy constraint. This dependence of the stochastic fluctuations on the environment is rooted in the cell mechanical activity. Indeed if $\chi_{\Sigma a} = 0$ (i.e. $\tau_a = \infty$), the relation fixing Θ is independent of λ as in these conditions,

$$\mu_0^2 = \frac{\Theta L \tau_r}{\alpha_{ab}^2} \left(\frac{1}{48} \left(\frac{6\tau_r}{\tau_d} - 3\sqrt{2} \sqrt{\frac{\tau_r}{\tau_d}} \left(4 \tanh\left(\sqrt{\frac{\tau_d}{2\tau_r}}\right) + \coth\left(\sqrt{\frac{\tau_d}{2\tau_r}}\right) + 77 \right) \right) \right)_{\tau_r/\tau_d \rightarrow 0} \rightarrow \frac{77\Theta L \tau_r}{48\alpha_{ab}^2}.$$

We show on Fig. 4 the value of Θ normalized by $\Theta_0 = \alpha_{ab}^2 \mu_0^2 / (L\tau_r)$ for several choices of τ_a . When τ_a is large compared to τ_r (i.e. the cell contractility is small), Θ is almost constant as a function of the external viscous friction Q_λ and assumes the value computed above. Outside of this limit, the value of Θ as a function of Q_λ emerging from the energy homeostatic constraint displays two plateau regions connected by a region of decrease. This region where Θ varies corresponds to a physiological range $Q_\lambda \in [10^{-10}, 1]$. The fact that, depending on the cell type, the glycolysis pathway is affected by the rigidity of the environment was recently demonstrated experimentally by [Park et al. \(2020\)](#).

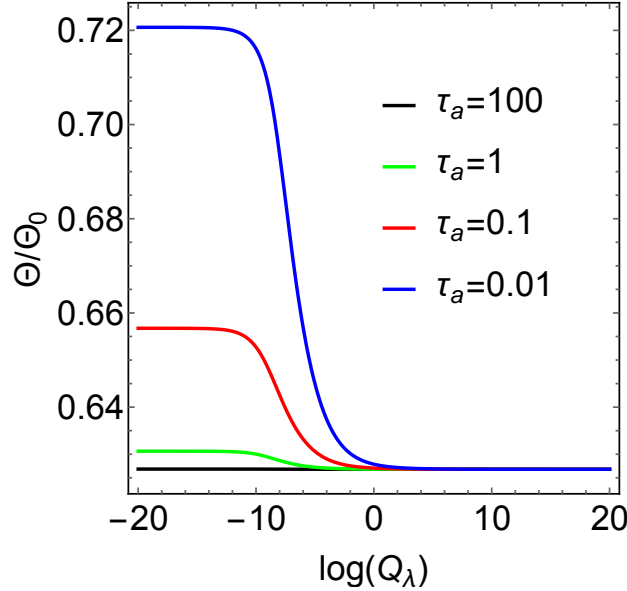


Figure 4: Amplitude of the fluctuations Θ controlling the energy homeostasis as a function of Q_λ , the friction with the external environment. Using the parameters in Table 2, we set: $\tau_d \approx 100$ s, $\tau_r \approx 0.04$ s, $L/l_0 \approx 530$ and $Q_\eta \approx 10^6$.

As experimental access to Θ is difficult, we now formulate more easily testable predictions by computing the center of mass fluctuations of the cell in our motility model.

4.4. Stochastic cell motion

Based on formula (22), we obtain the following expression relating cell velocity and $\Delta\mu_{ab}$:

$$V(t) = \frac{\chi_{\Sigma a} \Lambda^2 \operatorname{csch}\left(\frac{\Lambda L}{2}\right) \int_0^L \sinh\left(\Lambda\left(\frac{L}{2} - u\right)\right) \Delta\mu_{ab}(u, t) du}{\eta \Lambda^3 L - \lambda \Lambda L + 2\lambda \tanh(\Lambda L/2)}. \quad (32)$$

Clearly, when $\Delta\mu_{ab} = \Delta\mu_{ab}^0$ is constant, the cell velocity vanishes ($V = 0$) because our model does not sustain spontaneous polarization as in [Recho et al. \(2013\)](#). This is due to the fact that, for simplicity and to stay in the strict Onsager framework where kinetic coefficients are constants, we have not considered that the active contractile stress depends on the local concentration of molecular motors. However, in the presence of the metabolic fluctuations Γ , the cell velocity still undergoes non-trivial fluctuations as the same expression (32) relates V with $\delta\mu_{ab}$. Our model is designed to investigate the properties of such fluctuations.

To quantify the persistence and randomness of the cell motion ([Stokes et al., 1991](#); [Dieterich et al., 2008](#); [Petrie et al., 2009](#); [Maiuri et al., 2015](#)), we follow the classical path and define the variation of the cell position from its initial location by

$$\delta X(t) = \int_0^t V(u) du, \text{ and its associated mean square displacement } \text{MSD}(t) = \mathbb{E}(\delta X(t)^2).$$

Plugging (29) into (32) we express the velocity as a function of the $\delta\mu$ modes:

$$V(t) = \frac{2\sqrt{2/L}\chi_{\Sigma a}\Lambda}{\lambda} \sum_{k=0}^{\infty} \vartheta_{2k+1} \delta\mu_{2k+1}(t) \text{ where } \vartheta_k = \frac{f^2}{(f^2 + \pi^2 k^2)(fp - f + 2 \tanh(f/2))}.$$

Then, using the solution for the odd modes in (29) and the noise statistical property (30), we can express the MSD as

$$\text{MSD}(t) = \frac{64\Theta L \chi_{\Sigma a}^2 \Lambda^2}{\lambda^2 \alpha_{ab}^2 \pi^2} \int_0^t \int_0^t \int_0^t \int_0^t \delta(v - v') H(u - v) H(u' - v') \operatorname{tr}(\mathbb{A}_O(u - v, u' - v')) du du' dv dv',$$

where H denotes the Heaviside function and the operator \mathbb{A}_O reads

$$\mathbb{A}_O(u - v, u' - v') = \left(\mathbb{1} + \frac{e^{s(u-v)} - 1}{s} \mathbb{M}_O^T \right) e^{\mathbb{D}_O(u-v)} \bar{\vartheta}_O^T \bar{\vartheta}_O e^{\mathbb{D}_O(u'-v')} \left(\mathbb{1} + \frac{e^{s(u'-v')} - 1}{s} \mathbb{M}_O \right) \bar{\mathbb{D}}_O^{-1},$$

with the various quantities entering in the above expression defined in [Appendix B](#). We show in [Fig. 5](#) the typical scaling exponent a of the MSD as a function of time: $\text{MSD}(t) \sim t^a$. The cell motion is diffusive ($a = 1$) at both very short time and long timescales and undergoes a transition to super-diffusive ($1 \leq a \leq 2$) and hyper-ballistic ($a \geq 2$) motion in between. In [Dieterich et al. \(2008\)](#), based on experimental measurements of the positions of cells moving on a two-dimensional substrate, the authors report a similar qualitative behavior where the exponent of the MSD a reaches a maximum at an intermediate timescale.

The effective diffusion coefficient for cell motion at a long time scale defined as

$$D_{\text{eff}}^{\text{cell}} = \lim_{t \rightarrow \infty} \frac{\text{MSD}(t)}{2t},$$

takes a simple form:

$$D_{\text{eff}}^{\text{cell}} = \frac{4\alpha_{ab} l_0^2 \mu_0^2}{\tau_r \tau_a \eta} \frac{\Theta}{\Theta_0} \frac{p}{Q_\lambda} \sum_{k=0}^{\infty} \left(\frac{\vartheta_{2k+1}}{\pi(2k+1)d_{2k+1}} \right)^2. \quad (33)$$

Based on such a diffusion coefficient, we can compute a cell effective temperature using the Einstein-Smoluchowski relation:

$$T_{\text{eff}}^{\text{cell}} = \frac{\xi_{\text{eff}}^{\text{cell}} D_{\text{eff}}^{\text{cell}}}{k_B}, \quad (34)$$

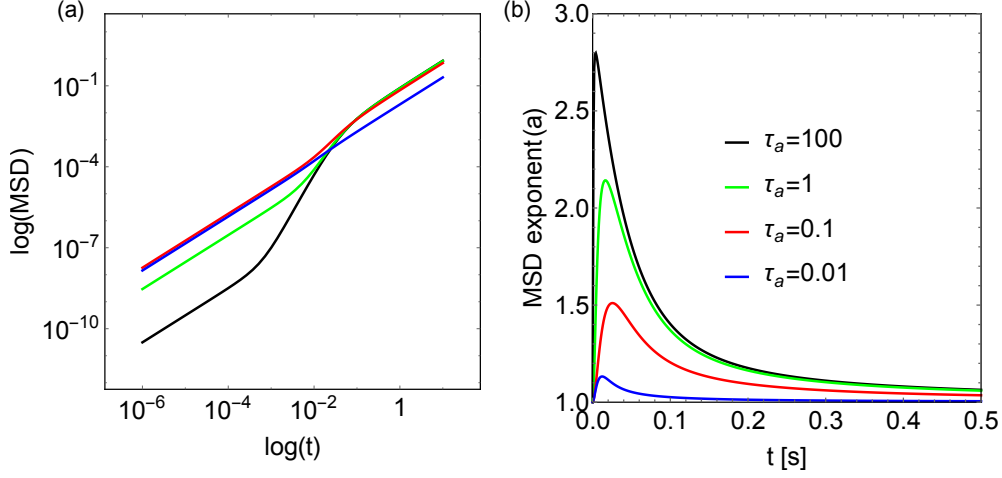


Figure 5: (a) Scaling in a log-log plot of the MSD with time for several values of τ_a . Two diffusive regimes at short and long timescales are connected by a super-diffusive regime at intermediate timescales. (b) Evolution with time of the exponent of the MSD $a = t\partial_t \text{MSD}(t)/\text{MSD}(t)$. Using the parameters in Table 2, we set: $\tau_d \approx 100\text{s}$, $\tau_r \approx 0.04\text{s}$, $L/l_0 \approx 530$, $Q_\eta \approx 10^6$ and $Q_\lambda \approx 10^{-4}$.

where $\xi_{\text{eff}}^{\text{cell}}$ is an effective cell friction coefficient with its environment that can be related to the local one by $\xi_{\text{eff}}^{\text{cell}} = \lambda w L h$ where w is the cell track width (so wL is the cell contact area) and h is the cell thickness. This effective temperature corresponds to the absolute temperature needed to obtain the observed fluctuations of the cell center of mass if the cell were a passive solid object in a thermal bath for which the fluctuation-dissipation relation (34) would apply. See Selmecki et al. (2008) for more details on this phenomenological link. We thus obtain

$$T_{\text{eff}}^{\text{cell}} = \frac{4wLh\alpha_{ab}\mu_0^2}{k_B\tau_r\tau_a} \frac{\Theta}{\Theta_0} p \sum_{k=0}^{\infty} \left(\frac{\vartheta_{2k+1}}{\pi(2k+1)d_{2k+1}} \right)^2. \quad (35)$$

Based on the rough estimates reported in Table 2, we can estimate using formula (33) the value of μ_0 such that the cell effective diffusive motion is realistic: $D_{\text{eff}}^{\text{cell}} \approx 10\mu\text{m}^2\text{s}^{-1}$ (Estabridis et al., 2018; Prahl et al., 2020; Maiuri et al., 2015). Doing so, we obtain $\mu_0 \approx 2 \times 10^6$ J/kg. Multiplying this quantity by the mass of ATP contained in a single cell (0.5×10^{-15} kg for an ATP concentration of 1mM), we estimate the total free energy of the cell to be 10^{-9} J which is line with the value reported in Shishvan et al. (2018). We can also estimate using (35) the typical effective temperature of a cell. Using the estimates of Table 2 and $\mu_0 \approx 2 \times 10^6$ J/kg, we obtain $T_{\text{eff}}^{\text{cell}} \approx 10^{10}$ K, again in agreement with Shishvan et al. (2018). Our model therefore provides a realistic explanation for the cell fluctuations of the center of mass which are rooted in the stochastic nature of the energy delivery to the molecular motors actuating the cytoskeleton.

We show on Fig. 6 the dependence of $D_{\text{eff}}^{\text{cell}}$ and $T_{\text{eff}}^{\text{cell}}$ on the parameter Q_λ quantifying the friction with the environment. When Q_λ is very large, the effective diffusion of the cell goes to zero while it reaches a plateau independent of the value of Q_λ for low friction. These two limiting behaviors are connected by a region (containing the range of physiological values of Q_λ) where $D_{\text{eff}}^{\text{cell}}$ changes with Q_λ . These variations are not necessarily monotonic depending of the value of τ_a . The effective temperature of the cell increases with Q_λ to reach a plateau region at high friction, where temperature becomes independent of the mechanical environment.

5. Discussion

We have presented a linear close-to-equilibrium formalism of cell mechanics coupling the active behaviour of its cytoskeleton with the metabolic pathways recycling the molecules delivering chemical energy into the system. A key assumption of our model is that this complex recycling process is effectively described by an equilibrium reservoir

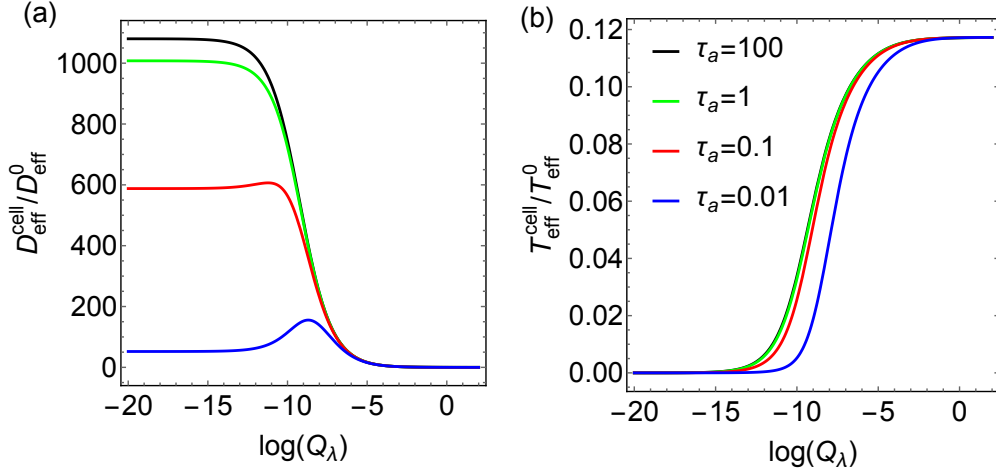


Figure 6: (a) Effective diffusion coefficient of the cell along its track as a function of the external friction. The normalization constant is $D_{\text{eff}}^0 = 4\alpha_{ab}\mu_0^2\tau_r^2l_0^2/(\tau_a\eta)$. (b) Effective temperature of the cell along its track as a function of the external friction. The normalization constant is $T_{\text{eff}}^0 = 4wLh\alpha_{ab}\mu_0^2\tau_r^2/(k_B\tau_a)$. Using the parameters in Table 2, we set: $\tau_d \approx 100\text{s}$, $\tau_r \approx 0.04\text{s}$, $L/l_0 \approx 530$ and $Q_\eta \approx 10^6$.

producing fluctuations whose magnitude is fixed by *energy homeostasis*, i.e. to insure that the chemo-mechanical free energy of the cell remains fixed regardless of the external mechanical conditions. As a result, we obtain a stochastic active gel model of the cytoskeleton which generalizes the deterministic approach of Jülicher et al. (2007).

We then apply this formalism to the model problem of a cell randomly migrating along a straight one-dimensional track. This simple example reveals that the fluctuations of the cell position and the fluctuations of the recycling process of the chemo-mechanical energy delivery are mechanically coupled through an Onsager cross coefficient at the origin of active contractile stress in the system. In particular, the model can explain how the metabolic fluctuations can be influenced by the mechanical forces applied on the cell in order to fulfill the energy homeostasis constraint. It also predicts, in agreement with experiments, that the statistical fluctuations of the cell position are diffusive at short and long timescales (with different effective diffusion coefficients) and that these two regimes are connected by a super-diffusive regime at intermediate timescales. The magnitude of the long timescale cell diffusion coefficient is in agreement with a rough estimate of the total cell energy resources. We also show how such a diffusion is modified by the external mechanical properties of the environment. In our simple model these are encapsulated in a single friction coefficient only. Depending on the magnitude of the active gel contractility, this diffusion coefficient can have a non-trivial maximum corresponding to an optimal friction coefficient where the cell mobility is maximal.

The linearity of our cell migration model allows us to obtain some results analytically, without having to rely on numerics but does not allow us to investigate some interesting instabilities. In particular, if we were to augment the model by considering distributions of molecular motors as in Recho et al. (2015), it would be able to generate a spontaneous polarization of the cell. The integration of such a property in the present formalism can be achieved by supposing that $\chi_{\Sigma_d}(c)$ depends on $c(y, t)$ the motor local concentration. It would lead to interesting predictions linking not only the velocity standard deviation but also the velocity average value and the statistics of the repolarization events with the stochasticity of the energy renewal process and the energy homeostasis. This could serve as a basis to justify from an active gel standpoint the effective phase-field theories presented in Prentice-Mott et al. (2016); Alonso et al. (2018); Moreno et al. (2020) and would also provide a potential theoretical background to justify the biological noise introduced in these theories. In the same vein, it would be natural to assume that the kinetic coefficient controlling the cell metabolism $\bar{k}_n(\Delta\mu)$ depends on $\Delta\mu$ as, for instance, energy is required for the performance of certain steps in the glycolysis or Krebs cycle. This would have the consequence that the environment mechanics will not only control the standard deviation of the rate at which glycolysis runs but also the mean of the rate as observed experimentally by Park et al. (2020). More work will be needed in the future to explore these issues.

6. Acknowledgments

This research project was initiated during the Summer School on ‘‘Cell Mechanobiology’’ held in September 2018 at CISM (Udine). A.D.S. acknowledges support from ERC (Advanced Grant 340685-MicroMotility). R.M.M. acknowledges support by the MRSEC Program NSF under Award No. DMR 1720256 (IRG-3). P.R. acknowledges support from a CNRS MOMENTUM grant. The authors are grateful to L. Truskinovsky for insightful and critical comments.

Appendix A. Justification of expression (24).

Given the quadratic form of the chemical free energy (11) we can directly relate the mass fractions with their associated chemical potentials such that $\partial_t x_i = \bar{x}_i \partial_t \mu_i / R_i$ and we can rewrite (23) using only the chemical potentials as variables:

$$\begin{aligned}\alpha_a \partial_t \mu_a &= M_a \partial_{yy} \mu_a + \chi_{\Sigma a} \partial_y v - k_{na} \Delta \mu_{ab} + v \bar{k}_n \Delta \mu_{np} + v \partial_t X \\ \alpha_b \partial_t \mu_b &= M_b \partial_{yy} \mu_b - \chi_{\Sigma a} \partial_y v + k_{na} \Delta \mu_{ab} - v \bar{k}_n \Delta \mu_{np} - v \partial_t X \\ \alpha_n \partial_t \mu_n &= M_n \partial_{yy} \mu_n + v \bar{k}_n \Delta \mu_{ab} - \bar{k}_n \Delta \mu_{np} - \partial_t X \\ \alpha_p \partial_t \mu_p &= M_p \partial_{yy} \mu_p - v \bar{k}_n \Delta \mu_{ab} + \bar{k}_n \Delta \mu_{np} + \partial_t X,\end{aligned}\tag{A.1}$$

where we have introduced the notations

$$k_{na} = v^2 \bar{k}_n + k_a \text{ and } \alpha_i = \rho_f (1 - \phi) \frac{\bar{x}_i}{R_i}.\tag{A.2}$$

The boundary conditions associated to (A.1) (see (9)) are no flux for a and b : $\partial_y \mu_{a,b}|_{0,L} = 0$ and imposed chemical potentials for n and p : $\mu_{n,p}|_{0,L} = \mu_{n,p}^0$. These last Dirichlet conditions correspond in (13) to the physical limit where the nutrients and products permeation coefficients $L_{n,p}$ are large while the products $j_{n,p} = L_{n,p}(\mu_{n,p}|_{0,L} - \mu_{n,p}^0)$, representing the incoming and outgoing fluxes for n and p , remain finite.

We first simplify the system (A.1) by approximating $\alpha_a \simeq \alpha_b \simeq \alpha_{ab} = (\alpha_a^{-1} + \alpha_b^{-1})^{-1}$ and $\alpha_n \simeq \alpha_p \simeq \alpha_{np} = (\alpha_n^{-1} + \alpha_p^{-1})^{-1}$. These assumptions rely on the value of the molar masses ($m_{ATP} = 507 \text{g/mol}$, $m_{ADP} = 427 \text{g/mol}$, $m_{glucose} = 180 \text{g/mol}$ and $m_{CO_2} = 44 \text{g/mol}$) and an estimate of the various species concentrations in the cell ($[ATP] = 0.7 \text{mM}$, $[ADP] = 0.2 \text{mM}$, $[glucose] = 0.5 \text{mM}$ and $[CO_2] = 1 \text{mM}$ for *Dictyostelium discoideum* (Albe et al., 1990; Blombach and Takors, 2015)) and lead to $\alpha_{ab} \simeq 10^{-5} \text{kg}^2 \text{m}^{-3} \text{J}^{-1}$ and $\alpha_{np} \simeq 5 \times 10^{-7} \text{kg}^2 \text{m}^{-3} \text{J}^{-1}$.

Similarly, we suppose that $M_a \simeq M_b \simeq M_{ab} = (M_a^{-1} + M_b^{-1})^{-1}$ and $M_n \simeq M_p \simeq M_{np} = (M_n^{-1} + M_p^{-1})^{-1}$ since the Stokes radii of a and b ($r_{ATP} \simeq r_{ADP} = 7 \times 10^{-10} \text{m}$) and n and p ($r_{glucose} = 3.8 \times 10^{-10} \text{m}$ and $r_{CO_2} = 2 \times 10^{-10} \text{m}$) are about the same. The resulting diffusion coefficients are $D_{np} = M_{np} / \alpha_{np} = k_B T / (6\pi r_{np} \eta_f) \simeq 1.5 \times 10^{-9} \text{m}^2 \cdot \text{s}^{-1}$ and $D_{ab} = M_{ab} / \alpha_{ab} = k_B T / (6\pi r_{ab} \eta_f) \simeq 3 \times 10^{-10} \text{m}^2 \cdot \text{s}^{-1}$. However, ATP and ADP are highly reactive which results in a trapping that effectively reduces their diffusion coefficient by one or two orders of magnitude (Saks et al., 2003). Having assumed that n and p as well as a and b have the same effective mobility in the cell, we conclude that

$$S_{ab} = \frac{\mu_a + \mu_b}{2} \text{ and } S_{np} = \frac{\mu_n + \mu_p}{2}$$

are constants fixed by the initial conditions and we can reduce (A.1) to a system of only two stochastic partial differential equations involving the difference of chemical potentials

$$\begin{aligned}\frac{\alpha_{ab}}{2} \partial_t \Delta \mu_{ab} &= \frac{M_{ab}}{2} \partial_{yy} \Delta \mu_{ab} + \chi_{\Sigma a} \partial_y v - k_{na} \Delta \mu_{ab} + v \bar{k}_n \Delta \mu_{np} + v \Gamma \\ \frac{\alpha_{np}}{2} \partial_t \Delta \mu_{np} &= \frac{M_{np}}{2} \partial_{yy} \Delta \mu_{np} + v \bar{k}_n \Delta \mu_{ab} - \bar{k}_n \Delta \mu_{np} - \Gamma,\end{aligned}\tag{A.3}$$

where $\Gamma(y, t) = \partial_t X(y, t)$ is a Gaussian process satisfying

$$\mathbb{E}(\Gamma(y, t)) = 0 \text{ and } \mathbb{E}(\Gamma(y, t) \Gamma(y', t')) = 2\Theta \min(y, y') \delta(t - t').$$

We now further simplify the above system (A.3) by neglecting the reaction term in (A.3)₂ compared to diffusion. This reduction is based on the fact that the diffusive length scale $(M_{np} / \bar{k}_n)^{1/2} \simeq 400 \mu\text{m}$ is an order of magnitude larger than the typical cell length ($10 \mu\text{m}$). To estimate \bar{k}_n we consider the global rate of ATP turnover in the cell k_n / α_{np} to

be 0.01 s^{-1} (Skog et al., 1982). We therefore approximate $\Delta\mu_{np} = \Delta\mu_{np}^0 + \bar{\Gamma}$, where $\bar{\Gamma}$ is a Gaussian noise satisfying the diffusion equation $\partial_t \bar{\Gamma} = D_{np} \partial_{yy} \bar{\Gamma} - (2/\alpha_{np}) \Gamma$ with Dirichlet boundary conditions. Since this equation is linear, it is clear that $\bar{\Gamma}$ remains Gaussian with a zero mean while its covariance can be directly related to Θ . Plugging this expression for $\Delta\mu_{np}$ into (A.3)₁, we obtain

$$\frac{\alpha_{ab}}{2} \partial_t \Delta\mu_{ab} = \frac{M_{ab}}{2} \partial_{yy} \Delta\mu_{ab} + \chi_{\Sigma a} \partial_y v - k_{na} \Delta\mu_{ab} + v \bar{k}_n \Delta\mu_{np}^0 + v(\Gamma + \bar{k}_n \bar{\Gamma}) \quad (\text{A.4})$$

which, differentiating relation (18) and using again the fact that $M_{np}/(\bar{k}_n L^2) \gg 1$ can be put in the final form:

$$\partial_t \Delta\mu_{ab} = D_{ab} \partial_{yy} \Delta\mu_{ab} + \frac{2k\chi_{\Sigma a}}{\alpha_{ab}(1-\phi)\eta_f} \partial_{yy} P_f - \frac{2k_{na}}{\alpha_{ab}} \Delta\mu_{ab} + \frac{2v\bar{k}_n}{\alpha_{ab}} \Delta\mu_{np}^0 + \frac{2v}{\alpha_{ab}} \Gamma. \quad (\text{A.5})$$

In the framework of the active segment, the energy homeostasis assumption (14) reads:

$$(1-\phi)\rho_f S \sum_{i=g,a,b,n,p} \frac{R_i}{2} \lim_{T \rightarrow \infty} \frac{1}{T} \int_0^T \int_0^L \mathbb{E} \left(\left(\frac{x_i - \bar{x}_i}{\bar{x}_i} \right)^2 \right) dy dt = F_0, \quad (\text{A.6})$$

where S is a unit surface equating the height of the cell (typically a few microns) multiplied by the thickness of the track (typically again a few microns). Based on the fact that $x_g = \bar{x}_g$, S_{ab} and S_{np} are fixed and $\mathbb{E}(\delta\mu_{ab}) = 0$, we can rewrite the condition (A.6) in a form that only involves $\mathbb{E}(\delta\mu_{ab}^2)$:

$$\lim_{T \rightarrow \infty} \frac{1}{LT} \int_0^T \int_0^L \mathbb{E}(\delta\mu_{ab}^2) dy dt = \mu_0^2, \quad (\text{A.7})$$

where μ_0^2 is a new constant.

Appendix B. Justification of expressions (29).

Using the Hilbert-Schmidt projection of $\delta\mu$, we express the entries of the last equation of system (27) as:

$$\begin{aligned} \partial_t \delta\mu(y, t) &= \sum_{k=0}^{\infty} \partial_t \delta\mu_k(t) w_k(y) \\ D_{ab} \partial_{yy} \delta\mu(y, t) &= -D_{ab} \sum_{k=0}^{\infty} \frac{k^2 \pi^2}{L^2} \delta\mu_k(t) w_k(y) \\ \frac{2k\chi_{\Sigma a}}{\alpha_{ab}\eta_f(1-\phi)} \partial_{yy} \delta P_f(y, t) &= \sum_{k=0}^{\infty} \alpha_k \delta\mu_k(t) w_k(y) + \sum_{k=0}^{\infty} \tilde{\alpha}_{2k+1} \delta\mu_{2k+1}(t) \sinh\left(\frac{\Lambda}{2}(L-2y)\right) = \\ &= \sum_{k=0}^{\infty} \alpha_k \delta\mu_k(t) w_k(y) + \sum_{k=0}^{\infty} \sum_{l=0}^{\infty} \tilde{\alpha}_{2k+1} \beta_{2l+1} \delta\mu_{2k+1}(t) w_{2l+1}(y) \end{aligned}$$

where,

$$\alpha_k = -\frac{2\pi^2 k^2}{\tau_a (\pi^2 k^2 + f^2)}, \quad \gamma_k = -\frac{4\sqrt{2/L} f^2 \text{sech}(f/2)}{\tau_a (\pi^2 k^2 + f^2) (pf - f + 2 \tanh(f/2))} \quad \text{and} \quad \beta_k = \frac{2\sqrt{2L} f \cosh(f/2)}{\pi^2 k^2 + f^2}.$$

We can therefore write two separate sets of linear first order ODE solving the even and odd modes of $\delta\mu$:

$$\forall k \geq 0, \quad \begin{aligned} \partial_t \delta\mu_{2k}(t) &= d_{2k} \delta\mu_{2k}(t) + \frac{2}{\alpha_{ab}} \Gamma_{2k}(t) \\ \partial_t \delta\mu_{2k+1}(t) &= d_{2k+1} \delta\mu_{2k+1}(t) + \beta_{2k+1} \sum_{l=0}^{\infty} \gamma_{2l+1} \delta\mu_{2l+1} + \frac{2}{\alpha_{ab}} \Gamma_{2k+1}(t), \end{aligned} \quad (\text{B.1})$$

where

$$d_k = -\frac{(\pi k)^2}{\tau_d} - \frac{2}{\tau_r} + \alpha_k.$$

To solve the system (B.1), we consider it up to a finite mode $0 \leq k \leq N$ and denote $\overline{\delta\mu}_E = (\delta\mu_{2k})_{k \geq 0}$ the vector of even modes of $\delta\mu$ and $\overline{\delta\mu}_O = (\delta\mu_{2k+1})_{k \geq 0}$ the vector of odd modes. More generally, the indices E and O will be used throughout the text to extract the even and odd components of a vector or a matrix. We can thus rewrite (B.1) in matrix form as

$$\partial_t \overline{\delta\mu}_E = \mathbb{D}_E \overline{\delta\mu}_E + \frac{2}{\alpha_{ab}} \overline{\Gamma}_E \quad \text{and} \quad \partial_t \overline{\delta\mu}_O = (\mathbb{D}_O + \mathbb{M}_O) \overline{\delta\mu}_O + \frac{2}{\alpha_{ab}} \overline{\Gamma}_O, \quad (\text{B.2})$$

where $\mathbb{D} = \text{diag}(\bar{d})$ is the diagonal matrix $\mathbb{D}_{ij} = d_i \delta_{ij}$ and $\mathbb{M} = \bar{\beta} \bar{\gamma}^T$ is the matrix mixing the odd modes, $\mathbb{M}_{ij} = \beta_i \gamma_j$. We can express $\mathbb{D} = -(\pi^2/\tau_d) \bar{\mathbb{D}} - (2/\tau_r) \mathbb{1} - (2\pi^2/\tau_a) \bar{\mathbb{D}} (\pi^2 \bar{\mathbb{D}} + f^2 \mathbb{1})^{-1}$ where $\bar{\mathbb{D}}_{ij} = i^2 \delta_{ij}$.

The steady state solutions of (B.2) are then given by,

$$\bar{\delta\mu}_E(t) = \frac{2}{\alpha_{ab}} \int_0^t e^{\mathbb{D}_E(t-u)} \bar{\Gamma}_E(u) du \text{ and } \bar{\delta\mu}_O(t) = \frac{2}{\alpha_{ab}} \int_0^t e^{(\mathbb{D}_O + \mathbb{M}_O)(t-u)} \bar{\Gamma}_O(u) du. \quad (\text{B.3})$$

For the even modes, as \mathbb{D}_E is diagonal, it is straightforward to compute the integral as the exponential directly reads,

$$\forall t, (e^{\mathbb{D}_E t})_{ij} = e^{d_i t} \delta_{ij}.$$

The computation of $e^{(\mathbb{D}_O + \mathbb{M}_O)t}$ requires more care. Since \mathbb{D}_O and \mathbb{M}_O do not commute, we use the Trotter-Kato formula

$$e^{(\mathbb{D}_O + \mathbb{M}_O)t} = \lim_{n \rightarrow \infty} \left(e^{\mathbb{D}_O t/n} e^{\mathbb{M}_O t/n} \right)^n.$$

Next, as $\forall k \geq 1$,

$$\mathbb{M}_O^k = (\bar{\beta} \bar{\gamma}^T)^k = s^{k-1} \mathbb{M}_O, \quad (\text{B.4})$$

where the scalar product s reads $s = \bar{\beta}^T \bar{\gamma}$, we obtain,

$$e^{\mathbb{M}_O t/n} = \sum_{k=0}^{\infty} \frac{(\mathbb{M}_O t/n)^k}{k!} = \mathbb{1} + \sum_{k=1}^{\infty} \left(\frac{t}{n} \right)^k \frac{\mathbb{M}_O^k}{k!} = \mathbb{1} + \frac{\mathbb{M}_O}{s} \sum_{k=1}^{\infty} \left(\frac{st}{n} \right)^k \frac{1}{k!} = \mathbb{1} + \frac{e^{st/n} - 1}{s} \mathbb{M}_O.$$

Injecting this expression in the Trotter-Kato formula we have

$$\left(e^{\mathbb{D}_O t/n} e^{\mathbb{M}_O t/n} \right)^n = e^{\mathbb{D}_O t} \left(\mathbb{1} + \frac{e^{st/n} - 1}{s} (e^{-\mathbb{D}_O t/n} \bar{\gamma}) (e^{\mathbb{D}_O t/n} \bar{\beta})^T \right)^n,$$

which we expand with the binomial formula and a property similar to (B.4) to reach

$$\left(e^{\mathbb{D}_O t/n} e^{\mathbb{M}_O t/n} \right)^n = e^{\mathbb{D}_O t} \left[\mathbb{1} + (e^{-\mathbb{D}_O t/n} \bar{\gamma}) (e^{\mathbb{D}_O t/n} \bar{\beta})^T \frac{e^{st/n} - 1}{s \tilde{s}_n(t)} \sum_{k=1}^n \binom{n}{k} \tilde{s}_n(t)^k \right],$$

where,

$$\tilde{s}_n(t) = \frac{e^{st/n} - 1}{s} (e^{\mathbb{D}_O t/n} \bar{\beta})^T (e^{-\mathbb{D}_O t/n} \bar{\gamma}).$$

Thus,

$$\left(e^{\mathbb{D}_O t/n} e^{\mathbb{M}_O t/n} \right)^n = e^{\mathbb{D}_O t} \left[\mathbb{1} + \frac{(e^{st/n} - 1)((1 + \tilde{s}_n(t))^n - 1)}{s \tilde{s}_n(t)} (e^{-\mathbb{D}_O t/n} \bar{\gamma}) (e^{\mathbb{D}_O t/n} \bar{\beta})^T \right]$$

and taking the limit when $n \rightarrow \infty$, we finally obtain

$$\forall t, e^{(\mathbb{D}_O + \mathbb{M}_O)t} = e^{\mathbb{D}_O t} \left(\mathbb{1} + \frac{e^{st} - 1}{s} \mathbb{M}_O \right). \quad (\text{B.5})$$

In the above formula, s can be computed explicitly:

$$s = - \sum_{k=0}^{\infty} \frac{16f^3}{\tau_a (\pi^2(2k+1)^2 + f^2)^2 (pf - f + 2 \tanh(f/2))} = \frac{(f - \sinh(f)) \text{sech}^2(f/2)}{\tau_a (fp - f + 2 \tanh(f/2))}.$$

In index notation, formula (B.3) therefore leads to the expressions given in the main paper:

$$\forall i \geq 0, \left\{ \begin{array}{l} \delta\mu_{2i}(t) = \frac{2}{\alpha_{ab}} \int_0^t e^{d_{2i}(t-u)} \Gamma_{2i}(u) du \\ \delta\mu_{2i+1}(t) = \frac{2}{\alpha_{ab}} \int_0^t e^{d_{2i+1}(t-u)} \Gamma_{2i+1}(u) du + \frac{2}{\alpha_{ab}s} \int_0^t e^{d_{2i+1}(t-u)} (e^{s(t-u)} - 1) \beta_{2i+1} \sum_{k=0}^{\infty} \gamma_{2k+1} \Gamma_{2k+1}(u) du. \end{array} \right.$$

References

- Albe, K.R., Butler, M.H., Wright, B.E., 1990. Cellular concentrations of enzymes and their substrates. *Journal of theoretical biology* 143, 163–195.
- Alberts, B., Johnson, A., Lewis, J., Raff, M., Roberts, K., Walter, P., 2002. *Molecular biology of the cell*. 4 ed., Garland Science Taylor & Francis Group.
- Alonso, S., Stange, M., Beta, C., 2018. Modeling random crawling, membrane deformation and intracellular polarity of motile amoeboid cells. *PLoS one* 13, e0201977.
- Alt, W., Dembo, M., 1999. Cytoplasm dynamics and cell motion: two-phase flow models. *Mathematical biosciences* 156, 207–228.
- Barnhart, E.L., Lee, K.C., Keren, K., Mogilner, A., Theriot, J.A., 2011. An adhesion-dependent switch between mechanisms that determine motile cell shape. *PLoS biology* 9.
- Blanch-Mercader, C., Casademunt, J., 2013. Spontaneous motility of actin lamellar fragments. *Physical review letters* 110, 078102.
- Blombach, B., Takors, R., 2015. CO₂-intrinsic product, essential substrate, and regulatory trigger of microbial and mammalian production processes. *Frontiers in bioengineering and biotechnology* 3, 108.
- Brangwynne, C.P., MacKintosh, F., Weitz, D.A., 2007. Force fluctuations and polymerization dynamics of intracellular microtubules. *Proceedings of the National Academy of Sciences* 104, 16128–16133.
- Buskermolen, A.B., Suresh, H., Shishvan, S.S., Vigliotti, A., DeSimone, A., Kurniawan, N.A., Bouten, C.V., Deshpande, V.S., 2019. Entropic forces drive cellular contact guidance. *Biophysical journal* 116, 1994–2008.
- Cadart, C., Venkova, L., Recho, P., Lagomarsino, M.C., Piel, M., 2019. The physics of cell-size regulation across timescales. *Nature Physics* URL: <https://doi.org/10.1038/s41567-019-0629-y>, doi:10.1038/s41567-019-0629-y.
- Callan-Jones, A., Voituriez, R., 2013. Active gel model of amoeboid cell motility. *New Journal of Physics* 15, 025022.
- Coussy, O., 2004. *Poromechanics*. John Wiley & Sons.
- De Groot, S.R., Mazur, P., 2013. *Non-equilibrium thermodynamics*. Courier Corporation.
- Dieterich, P., Klages, R., Preuss, R., Schwab, A., 2008. Anomalous dynamics of cell migration. *Proceedings of the National Academy of Sciences* 105, 459–463.
- Dreher, A., Aranson, I.S., Kruse, K., 2014. Spiral actin-polymerization waves can generate amoeboidal cell crawling. *New Journal of Physics* 16, 055007.
- Edelstein-Keshet, L., Holmes, W.R., Zajac, M., Dutot, M., 2013. From simple to detailed models for cell polarization. *Philosophical Transactions of the Royal Society B: Biological Sciences* 368, 20130003.
- Edwards, S.F., Oakeshott, R., 1989. Theory of powders. *Physica A: Statistical Mechanics and its Applications* 157, 1080–1090.
- Engler, A.J., Sen, S., Sweeney, H.L., Discher, D.E., 2006. Matrix elasticity directs stem cell lineage specification. *Cell* 126, 677–689.
- Estabridis, H.M., Jana, A., Nain, A., Odde, D.J., 2018. Cell migration in 1d and 2d nanofiber microenvironments. *Annals of biomedical engineering* 46, 392–403.
- Fabry, B., Maksym, G.N., Butler, J.P., Glogauer, M., Navajas, D., Fredberg, J.J., 2001. Scaling the microrheology of living cells. *Physical review letters* 87, 148102.
- Giomi, L., DeSimone, A., 2014. Spontaneous division and motility in active nematic droplets. *Physical review letters* 112, 147802.
- Gupta, M., Sarangi, B.R., Deschamps, J., Nematbakhsh, Y., Callan-Jones, A., Margadant, F., Mège, R.M., Lim, C.T., Voituriez, R., Ladoux, B., 2015. Adaptive rheology and ordering of cell cytoskeleton govern matrix rigidity sensing. *Nature communications* 6, 1–9.
- Howard, J., et al., 2001. *Mechanics of motor proteins and the cytoskeleton*. Sinauer associates Sunderland, MA.
- Jülicher, F., Kruse, K., Prost, J., Joanny, J.F., 2007. Active behavior of the cytoskeleton. *Phys. Rep.* 449, 3–28. doi:<http://dx.doi.org/10.1016/j.physrep.2007.02.018>.
- Kimpton, L., Whiteley, J., Waters, S., Oliver, J., 2015. On a poroviscoelastic model for cell crawling. *Journal of mathematical biology* 70, 133–171.
- Kruse, K., Joanny, J.F., Jülicher, F., Prost, J., Sekimoto, K., 2005. Generic theory of active polar gels: a paradigm for cytoskeletal dynamics. *The European Physical Journal E* 16, 5–16.
- Li, L., Nørrelykke, S.F., Cox, E.C., 2008. Persistent cell motion in the absence of external signals: a search strategy for eukaryotic cells. *PLoS one* 3, e2093.
- Maiuri, P., Rupprecht, J.F., Wieser, S., Rupprecht, V., Bénichou, O., Carpi, N., Coppey, M., De Beco, S., Gov, N., Heisenberg, C.P., et al., 2015. Actin flows mediate a universal coupling between cell speed and cell persistence. *Cell* 161, 374–386.
- Maiuri, P., Terriac, E., Paul-Gilloteaux, P., Vignaud, T., McNally, K., Onuffer, J., Thorn, K., Nguyen, P.A., Georgoulia, N., Soong, D., et al., 2012. The first world cell race. *Current Biology* 22, R673–R675.
- Moeendarbary, E., Valon, L., Fritzsche, M., Harris, A.R., Moulding, D.A., Thrasher, A.J., Stride, E., Mahadevan, L., Charras, G.T., 2013. The cytoplasm of living cells behaves as a poroelastic material. *Nature materials* 12, 253.
- Moreno, E., Flemming, S., Font, F., Holschneider, M., Beta, C., Alonso, S., 2020. Modeling cell crawling strategies with a bistable model: From amoeboid to fan-shaped cell motion. *Physica D: Nonlinear Phenomena*, 132591.
- Nadrowski, B., Martin, P., Jülicher, F., 2004. Active hair-bundle motility harnesses noise to operate near an optimum of mechanosensitivity. *Proceedings of the National Academy of Sciences* 101, 12195–12200.
- Park, J.S., Burckhardt, C.J., Lazcano, R., Solis, L.M., Isogai, T., Li, L., Chen, C.S., Gao, B., Minna, J.D., Bachoo, R., et al., 2020. Mechanical regulation of glycolysis via cytoskeleton architecture. *Nature* 578, 621–626.
- Parsons, J.T., Horwitz, A.R., Schwartz, M.A., 2010. Cell adhesion: integrating cytoskeletal dynamics and cellular tension. *Nature reviews Molecular cell biology* 11, 633–643.
- Petrie, R.J., Doyle, A.D., Yamada, K.M., 2009. Random versus directionally persistent cell migration. *Nature reviews Molecular cell biology* 10, 538–549.
- Pollard, T.D., Earnshaw, W.C., Lippincott-Schwartz, J., Johnson, G., 2016. *Cell Biology*. Elsevier Health Sciences.
- Prager-Khoutorsky, M., Lichtenstein, A., Krishnan, R., Rajendran, K., Mayo, A., Kam, Z., Geiger, B., Bershadsky, A.D., 2011. Fibroblast polarization is a matrix-rigidity-dependent process controlled by focal adhesion mechanosensing. *Nature cell biology* 13, 1457–1465.

- Prahl, L.S., Stanslaski, M.R., Vargas, P., Piel, M., Odde, D.J., 2020. Predicting confined 1d cell migration from parameters calibrated to a 2d motor-clutch model. *Biophysical journal*.
- Prentice-Mott, H.V., Meroz, Y., Carlson, A., Levine, M.A., Davidson, M.W., Irimia, D., Charras, G.T., Mahadevan, L., Shah, J.V., 2016. Directional memory arises from long-lived cytoskeletal asymmetries in polarized chemotactic cells. *Proceedings of the National Academy of Sciences* 113, 1267–1272.
- Prost, J., Jülicher, F., Joanny, J.F., 2015. Active gel physics. *Nature physics* 11, 111–117.
- Recho, P., Joanny, J.F., Truskinovsky, L., 2014. Optimality of contraction-driven crawling. *Physical Review Letters* 112, 218101.
- Recho, P., Putelat, T., Truskinovsky, L., 2013. Contraction-driven cell motility. *Physical review letters* 111, 108102.
- Recho, P., Putelat, T., Truskinovsky, L., 2015. Mechanics of motility initiation and motility arrest in crawling cells. *Journal of the Mechanics and Physics of Solids* 84, 469–505.
- Roux, C., Duperray, A., Laurent, V.M., Michel, R., Peschetola, V., Verdier, C., Étienne, J., 2016. Prediction of traction forces of motile cells. *Interface focus* 6, 20160042.
- Rubinstein, B., Fournier, M.F., Jacobson, K., Verkhovskiy, A.B., Mogilner, A., 2009. Actin-myosin viscoelastic flow in the keratocyte lamellipod. *Biophys. J.* 97, 1853–1863.
- Saks, V., Kuznetsov, A., Andrienko, T., Usson, Y., Appaix, F., Guerrero, K., Kaambre, T., Sikk, P., Lemba, M., Vendelin, M., 2003. Heterogeneity of adp diffusion and regulation of respiration in cardiac cells. *Biophysical Journal* 84, 3436–3456.
- Sekimoto, K., 2010. *Stochastic energetics*. volume 799. Springer.
- Selmecci, D., Li, L., Pedersen, L.I., Nrelykke, S., Hagedorn, P.H., Mosler, S., Larsen, N.B., Cox, E.C., Flyvbjerg, H., 2008. Cell motility as random motion: A review. *The European Physical Journal Special Topics* 157, 1–15.
- Shishvan, S., Vigliotti, A., Deshpande, V., 2018. The homeostatic ensemble for cells. *Biomechanics and modeling in mechanobiology* 17, 1631–1662.
- Skog, S., Tribukait, B., Sundius, G., 1982. Energy metabolism and atp turnover time during the cell cycle of ehrlich ascites tumour cells. *Experimental cell research* 141, 23–29.
- Solon, J., Levental, I., Sengupta, K., Georges, P.C., Janmey, P.A., 2007. Fibroblast adaptation and stiffness matching to soft elastic substrates. *Biophysical journal* 93, 4453–4461.
- Stankevics, L., Ecker, N., Terriac, E., Maiuri, P., Schoppmeyer, R., Vargas, P., Lennon-Duménil, A.M., Piel, M., Qu, B., Hoth, M., et al., 2020. Deterministic actin waves as generators of cell polarization cues. *Proceedings of the National Academy of Sciences* 117, 826–835.
- Stokes, C.L., Lauffenburger, D.A., Williams, S.K., 1991. Migration of individual microvessel endothelial cells: stochastic model and parameter measurement. *Journal of cell science* 99, 419–430.
- Suresh, S., 2007. Biomechanics and biophysics of cancer cells. *Acta biomaterialia* 3, 413–438.
- Suzuki, R., Hotta, K., Oka, K., 2015. Spatiotemporal quantification of subcellular atp levels in a single hela cell during changes in morphology. *Scientific reports* 5, 1–9.
- Tjhung, E., Marenduzzo, D., Cates, M.E., 2012. Spontaneous symmetry breaking in active droplets provides a generic route to motility. *Proceedings of the National Academy of Sciences* 109, 12381–12386.